**Nationaal Lucht- en Ruimtevaartlaboratorium**
National Aerospace Laboratory NLR

NLR-TP-97517

# Anechoic wind tunnels

H.H. Brouwer

# DOCUMENT CONTROL SHEET

| | ORIGINATOR'S REF.<br>NLR TP 97517. U | | SECURITY CLASS.<br>Unclassified |
|---|---|---|---|

ORIGINATOR
National Aerospace Laboratory NLR, Amsterdam, The Netherlands

TITLE
Anechoic Wind Tunnels

PRESENTED AT
The VKI Lecture Series "Aeroacoustics and Active Noise Control", 15-18 September 1997, Rhode-Saint-Genèse, Belgium

| AUTHORS | DATE | pp | ref |
|---|---|---|---|
| H.H. Brouwer | 970915 | 39 | 18 |

DESCRIPTORS

| | | |
|---|---|---|
| Acoustic measurement | Anechoic chambers | Wind tunnel apparatus |
| Acoustic properties | Helicopters | Wind tunnels |
| Aeroacoustics | High speed | Wind tunnel tests |
| Aerodynamic noise | Propeller noise | |
| Aircraft noise | Rail transportation | |

ABSTRACT
In this paper an overview is given of the most important aspects of acoustically treated wind tunnels and aeroacoustic testing in such tunnels. The requirements with respect to background noise and sound reflection by the tunnel walls are considered. The acoustic design of some large facilities is described, as well as some aspects of the acoustic measurement techniques applied in these tunnels. Finally, a number of typical applications is described.

217-02

**Summary**

In this paper an overview is given of the most important aspects of acoustically treated wind tunnels and aeroacoustic testing in such tunnels. The requirements with respect to background noise and sound reflection by the tunnel walls are considered. The acoustic design of some large facilities is described, as well as some aspects of the acoustic measurement techniques applied in these tunnels. Finally, a number of typical applications is described.

## Contents



1 Table
35 Figures

(39 pages in total)

## 1 Introduction

By definition, aeroacoustics always involves both sound and flow. The flow can be both internal, e.g. pipelines and valves, or external, e.g. around an aircraft. In this paper we limit ourselves to external flow problems. The research on aircraft noise is probably the most extensive application of aeroacoustics, but also the research on the noise made by cars, high-speed trains and wind turbines is worth mentioning as examples of aeroacoustics with external flows.

For meaningful experimental research the presence of flow is of paramount importance. One way of achieving this is to perform measurements at full scale. Indeed, in aeronautics flight tests are an indispensable part of a development programme. Also with respect to the other examples given above full scale tests are by no means exceptional, such as noise measurements along railway tracks, or near wind turbines. Such measurements, however, have some obvious drawbacks:

- In the case of flight measurements the costs are extremely high.
- If the tests are part of a program to design a new product, a prototype is not available before the program is nearly finished. It is a very unpleasant surprise if full scale tests reveal the need for significant design changes.
- Full scale sound measurements are usually performed in the open field, where changing weather conditions can have a ruinous effect on the reproducibility of the results. For example the noise made by wind turbines not only depends heavily on the wind force, but also, depending on the terrain, on the wind direction.
- To understand aeroacoustic phenomena, a detailed knowledge of the flow is essential. It can be extremely difficult to obtain such knowledge in the open field.

Therefore, aeroacoustic testing is usually done in wind tunnels on scale models, like most other experiments involving external air flow (i.e. external to the model). Most wind tunnels, however, are not suitable for acoustic measurements. In this paper an overview will be given of the most important aspects of acoustically treated wind tunnels and aeroacoustic testing in such tunnels.

## 2 Requirements and design

Wind tunnels in which acoustic measurements are performed have to satisfy at least the following two conditions: 1) The background noise must be significantly less than the noise one is interested in, and 2) The sound reflected by the tunnel walls should not spoil the sound field emitted directly by the source. The quantification of these conditions depend in principal on the specific test, but during the design phase of a new wind tunnel, or of a tunnel modification, upper limits have to be specified for both the background noise and the reflections.

### 2.1 Background noise

Background noise is the noise that is generated by the wind tunnel and the tunnel flow itself, i.e. the noise that is measured in the empty test section. This noise can have components that are of mechanical origin, e.g. the motor, or of aerodynamic origin.The main sources of aeroacoustic noise are the fan and the interaction of turbulent flow with structures.

In the case of an axial fan, low-frequency discrete tones are generated by the aerodynamic interaction between the rotating fan blades and the stator vanes. Stator vanes are non-rotating airfoils, usually mounted at a short distance downstream of the fan, see figure 1. The stator reduces the swirl that is generated by the fan, which increases the efficiency. The wakes of the fan blades impinge periodically on the stator vanes, generating pressure fluctuations on these vanes. These pressure fluctuations are the source of tonal noise. One of the most effective ways to reduce this noise is to make use of the cut-off properties of sound propagation in ducts. A sound pattern with a specific periodicity in circumferential direction cannot propagate if the frequency is lower than the so-called cut-off frequency, and will die out exponentially. The cut-off frequency depends on the periodicity, the sound pattern rotation speed, and the axial flow speed. In the case of interaction noise as described above, the periodicity is determined by the numbers of fan blades and stator vanes (Ref. 1). By tuning these numbers it is possible to eliminate the Blade Passing Frequency tone completely, as has been common practice in the design of turbofan engines in the last few decades. A second method to reduce this noise is to apply sweep to the blades and/or the vanes, see figure 2. Sweep introduces a variation in phase in spanwise direction, causing destructive interference in the pressure field.

Besides tonal noise, the fan also generates broadband noise, which is can be generated by turbulent inflow, the movement of the tips through the wall boundary layer, or when the flow over the blades is separated. The level of this noise depends heavily on the velocity of the flow relative to the blade. Therefore, the rotational speed of the fan should be kept as low as possible. In some anechoic wind tunnels a centrifugal fan is applied, which is not as efficient as an axial fan, but the fan noise is somewhat shielded from the flow duct, see figure 3.

Apart from noise reduction at the source, possibilities exist to absorb the noise as it propagates from the fan to the test section. In some wind tunnels one has used the turning vanes, which are mounted in the corners of the tunnel to maintain a smooth flow, for the installation of acoustic linings. The lining usually consists of a layer of bulk-absorbing material covered by a perforated metal sheet. These linings absorb a great deal of the fan noise, at the cost of a slight increase of power consumption.

In the case of an open test section, see figure 4, an other noise source is the turbulence in the shear layer coming from the nozzle, especially the interaction of the vortices in the shear layer with the edge of the nozzle. The generation of this noise can be reduced by installing flanges or protrusions on the nozzle, see figure 5. A recent investigation on this, where a noise reduction of 4 to 6 dB was achieved, is reported in reference 2.

### 2.2 Anechoic Environment

The purpose of most acoustic experiments in wind tunnels is to simulate noise sources in an open space, which means that at measurement positions the level of the sound reflected by the tunnel walls should be negligible with respect to the directly emitted sound. Chambers that satisfy this condition are called anechoic. In anechoic chambers the acoustic pressure $p$ behaves in the far field, i.e. at a distance $r$ which is much larger than the wavelength $\lambda$, as $1/r$, and thus is the acoustic intensity proportional to $1/r^2$. This so-called $1/r^2$ law is often used as a check on the anechoicity.

The means that are available to achieve an anechoic testing environment in a wind tunnel, depend on the type of tunnel. In the case of low speed wind tunnels one has the choice to construct an open or a closed test section. An open test section, see figure 4, has a number of advantages as compared to a closed test section with the same dimensions of the contraction:

- The walls of the hall enclosing the open jet are at greater distance from the sources.
- A better acoustic lining of the walls is possible (see below).
- Microphones can be placed outside the flow, thus avoiding aerodynamically generated microphone self-noise.

The standard acoustic lining for anechoic chambers consists of arrays of foam wedges. Such wedges are also applied in anechoic wind tunnels, but only in the case of an open test section, where the flow velocity at the walls of the testing hall is very low. The geometry of the wedges cause that the acoustic impedance, experienced by a sound wave impinging on the wall, is varying continuously from the top of the wedges to the base. In this way stepwise changes, which cause strong reflections, are avoided. The design of such a liner involves a choice for the dimensions, the material, and the relative positioning of the wedges. The main acoustic requirement for a design is specified in terms of the cut-off frequency, usually defined as the frequency at which 99 % of the acoustic power of a plane wave at normal incidence is absorbed, which can be achieved by choosing the right dimensions (longer wedges lead to a lower cut-off frequency) and a suitable value for the flow resistance of the material. Design charts based on experimental work are available for such an exercise, see e.g. reference 3. The design process may be optimized by the application of a finite element analysis, such as reported in reference 4 (Fig. 6).

Also some drawbacks of open test sections exist:

- More power is needed to achieve the same flow velocity.
- Sometimes low frequency flow vibrations, known as ‘pumping', occur.
- The core of uniform flow is smaller, as the shear layer from the nozzle increases in thickness with increasing distance from the nozzle edge.
- As mentioned above, the shear layer increases the background noise.

The phenomenon of pumping, if it occurs, sets the maximum speed at which the tunnel can be operated safely. Although several low frequency resonance mechanisms are possible (see Ref. 5), the one that is most closely associated with open test sections is caused by a feed-back between nozzle and collector. Vortices shed at the trailing edge of the nozzle impinge on the collector, where they generate acoustic waves, which propagate upstream and trigger the shedding of vortices at the nozzle. Similar methods as mentioned for the reduction of shear layer noise, i.e. the application of flanges or serrations (in this case mounted to the nozzle edge or the collector), may be used to avoid this phenomenon.

In the case of a closed test section the application of wedges is not feasible. If wedges could be found that survive insertion in a flow of, say, Mach 0.2, the quality of the flow itself would be spoiled dramatically, not to speak of the very high background noise levels that would be generated. The acoustic lining of closed test sections generally consists of a layer of bulk-absorbing material covered by a perforated sheet. Compared to wedges of the same dimensions the absorption is less effective.

High-speed wind tunnels, used for aerospace research in transonic or supersonic flows, always have closed test sections, for obvious reasons. The few high-speed wind tunnels that have an acoustic treatment have thus acoustic linings of the type described in the previous paragraph.

## 3 Characteristics of some anechoic wind tunnels

In this section the main characteristics are given of a rather arbitrary choice of acoustically treated wind tunnels. This choice includes the largest facilities in use by the aerospace industry. In section 5.5 wind tunnels in use by the car industry will be discussed.

### 3.1 The German-Dutch Wind Tunnel DNW

One of the largest anechoic facilities in the world is the German-Dutch Wind Tunnel DNW, see figure 7, located in the Noordoostpolder, The Netherlands. It is a low speed wind tunnel with three interchangeable, variable slotted wall test sections and an open jet (i.e. open test section) configuration. The open jet configuration is one of the design features adopted to make the DNW suitable for aeroacoustic testing. In this configuration the dimensions of the nozzle are 8 × 6 $m^2$ and the maximum velocity is 85 m/s. The length of the open jet is 20 m, the testing hall is 45 m × 30 m × 20 m (l×w×h).

Other aeroacoustic features are:

Low noise fan:

- Attached flow under all stationary test conditions.
- Stator vanes and nose cone supports have 15° sweep.
- Low tip speed.

Fan noise attenuation:

- Turning vanes upstream and downstream of the test section covered with acoustic lining.

Lining of testing hall:

- 40 % (primary reflections): Glass wool wedges with a base of 0.2 m × 0.2 m and a height of 0.8 m.
  Absorption coefficient 0.99, cut-off frequency 100 Hz.
- 60 % (secondary reflections): Flat material of 0.2 m thickness.
  Absorption coefficient 0.9, cut-off frequency 200 Hz.

The background noise of the DNW, measured with an out-of-flow microphone at 80 m/s, is below 80 dB in the 125 Hz 1/3 octave band and decreasing at higher frequencies, see figure 8. The anechoicity of the testing hall is illustrated in figure 9, where the decay of a sound field, generated by a source in the centre of the test section, is compared to the $1/r^2$ law, see section 2.2.

### 3.2 The CEPRA 19

The CEPRA 19 is a low speed wind tunnel, located in Orsay, France, specifically designed for aeroacoustic testing. It is an open test section wind tunnel (Fig. 10), with two interchangeable, circular nozzles: one with a diameter of 2 m, with maximum velocity 127 m/s, and one with a diameter of 3 m, with maximum velocity 70 m/s. The test chamber has the shape of the quarter of a sphere with a radius of 9.6 m. The main acoustic features are:

Fan:

- Centrifugal type.

Fan noise attenuation:

- Muffler with absorbing panels between test chamber and fan (Figs. 10 and 11).

Acoustic treatment of test chamber:

- Absorbing wedges of 0.8 m long on walls and ground,
- Exhaust bellmouth of perforated sheet (Fig. 11).

The resulting background noise levels (OASPL from 200 Hz to 80 kHz, measured with an out-of-flow microphone) and anechoicity are shown in figures 12 and 13. The practical frequency range is 100 Hz to 60 kHz.

### 3.3 The ARA Transonic Wind Tunnel

The ARA TWT is a conventional closed circuit type of wind tunnel, located at Bedford, UK, with a test section of 2.74 m × 2.44 m and a maximum Mach number of 1.4. To enable the measurement of propeller noise an acoustic insert was designed for the test section. This removable insert has a foam lining with a thickness of 0.15 m. The foam is covered with a 4 mm aluminium sheet of 37 % porosity, see figures 14 and 15.

This insert reduces the test section dimensions to 2.44 m × 2.13 m and the maximum Mach number to 0.8. A high level of anechoicity has been obtained in the frequency range of interest, specified as 570 Hz and higher, up to a Mach number of 0.6.

### 3.4 The S1MA Wind Tunnel

The ONERA S1MA wind tunnel located in Modane, France, is one of the largest transonic facilities in the world. It has a circular test section of 8 m diameter and the Mach number is continuously variable from 0.05 to 1. An acoustic lining exists for tunnel speeds up to Mach 0.35, a lining for tests up to Mach 0.85 is under construction.

This new lining consists of 0.15 m open cell foam covered by a 4 mm plate of 45 % porosity. The absorption coefficient at normal incidence is higher than 0.9 in the 315 Hz band, see figure 16. The test section will be become a little smaller, 6.9 m wide, 7 m high, and 8.5 m long, and will have an octagonal shape.

### 3.5 The NASA Ames 40×80 Foot Subsonic Wind Tunnel

The 40×80 Foot Subsonic Wind Tunnel at NASA Ames Research Center is probably the largest acoustically treated wind tunnel in the world. In the (closed) test section (12.2 m × 24.4 m) a maximum velocity of 116 m/s can be reached. A 0.15 m thick lining allows for acoustic measurements above 1000 Hz. In reference 6 a number of modifications are described which reduced the background noise, such as the installation of a new fan. The resulting background noise levels, measured with an in-flow microphone, are given in figure 17.

# 4 Measurement techniques

## 4.1 Scaling

Although some wind tunnels are large enough for full scale measurements on cars, trucks, small aircraft, etc., the vast majority of wind tunnel tests are carried out on scale models. Each discipline, i.e. aerodynamics, aeroelasticity, or aeroacoustics, has its own scaling rules.

In aeroacoustics, if the sound consists of discrete tones generated by rotating aerofoils, e.g. propellers, fans, or helicopter rotors, the scaling is quite easy. Let's take as an example an isolated propeller of 3 m diameter and a rotational speed of 1000 RPM at full scale. The noise generated by a propeller mainly consists of the Blade Passing Frequency tone and harmonics. If our propeller has f.i. six blades, it will generate tones of 100 Hz, 200 Hz, 300 Hz, etc. Suppose that a wind tunnel model of this propeller has a diameter of 0.75 m, or a scale of 1:4. Like in all wind tunnel testing where compressibility is the dominating phenomenon, the tunnel Mach number should be the same as the flight Mach number *M*. The local undisturbed Mach number relative to a propeller blade section is given by:

$$M_l = \sqrt{M^2 + \left(\Omega r / c_0\right)^2}$$

where $\Omega$ is the angular frequency, *r* is the radius of the blade section, and $c_0$ is the speed of sound.

This Mach number determines the aerodynamics and thus the pressure distribution on the blades, and it should be the same as in full scale. As *r* is scaled down by a factor 4, $\Omega$ has to be scaled up by the same factor, and the rotational speed becomes 4000 RPM. (For the moment we disregard differences in temperature and air density.) This is a general rule in aeroacoustics: frequencies should be scaled up by the same factor as the dimensions are scaled down, leaving the ratio of wavelength to model dimension the same. In the case of propeller noise there is a weak dependency of the noise on the Reynolds number through the pressure distribution, otherwise the simulation is exact. This means that, in the case of this example, the same noise level that would be found at a distance of 4 m, in some direction, from the full scale propeller, will be found at a distance of 1 m, in the same direction, from the model propeller, with frequencies of 400 Hz, 800 Hz, 1200 Hz, etc.

In case the temperature and the density of air in the wind tunnel differ from the situation to be simulated, some straightforward corrections have to be applied, based on the fact that $c_0$ is proportional to $\sqrt{T_0}$ and that the pressure scales on $\rho_0 c_0^2$, where $T_0$ and $\rho_0$ are the temperature and density of the undisturbed flow. The same scaling rules apply to the acoustic testing of turbomachinery and helicopter rotors.

Discrete tone may also be caused by periodic phenomena in separated flows. The most classical example of this is the aeolian tone, radiated by the flow across a circular cylinder. A detailed description of this phenomenon can be found in reference 7. The two major parameters involved are the Strouhal number, $fd/U_\infty$, and the Reynolds number, $dU_\infty/\nu$, where $f$ is the frequency of the tone, $d$ is the diameter of the cylinder, $U_\infty$ is the flow velocity, and $\nu$ is the kinematic viscosity. Over a wide range of the Reynolds number the Strouhal number of the aeolian tone is close to 0.2, meaning that the frequency scales with the inverse of the dimension, just as above. Unfortunately, no such simple rule exists for the sound intensity of aeolian tones. The intensity not only depends on Reynolds number but also on details like surface roughness and upstream turbulence.

Things become even more complicated with broadband noise, although the basic rule, that the frequencies generally scale with the inverse of the dimensions, remains valid. A wide variety of generation mechanisms exists, of which the interaction of a turbulent boundary layer with a trailing edge, an important source of wind turbine noise, and shear layer mixing noise, the major component of subsonic jet noise, are only two examples. The fact that translation to full scale can be difficult is by no means a reason to refrain from scaled wind tunnel experiments on such noise sources. On the contrary, such experiments are indispensable for the understanding of the mechanisms and for the determination of scaling laws.

### 4.2 Microphones

With acoustic measurements in an open test section, the first choice to be made with regard to the microphone positions is to place them outside or inside the flow. Both possibilities have their advantages and disadvantages.

Out-of-flow positioning has the disadvantage that the distance between microphone and source is relatively large, which has a negative effect on the signal-to-noise ratio, and that a correction has to be applied for the refraction of the sound by the shear layer. This correction is usually based on Amiet’s model for infinitely thin shear layers, see reference 8.

In-flow measurement has the disadvantage that the microphone and its support scatter the sound coming from the model and, even worse, generate extra noise by disturbing the flow. Hydrodynamic pressure fluctuations in the flow over the microphones are picked up by the membranes and cause extra noise in the microphone signal.

To reduce the microphone self-noise, nose cones, also called aerodynamic microphone forebodies, have to be used. In many cases commercially available nose cones, such as made by Brüel and Kjær, prevent self-noise sufficiently. However, these nose cones cause some additional peaks in the sound spectrum in the high frequency regime, see figure 18, and acoustic research on scale models requires analysis in this regime, see section 4.2. Therefore, extensive research on the mechanisms of microphone self-noise and means to reduce it is carried out, both in Europe (Ref. 9) and the USA (Ref. 10).

A nose cone consists of a cylindrical body with an aerodynamic contour, with screen covered apertures at some distance downstream of the nose.

There are several phenomena that may attribute to the generation of self-noise:

- Instabilities in the boundary layer, in the onset of transition from laminar to turbulent flow, generate pressure fluctuations which, if they occur at the location of the apertures, are picked up by the microphone. This problem is enhanced if cross-flow occurs, i.e. if the axis of the probe is not aligned with the local flow.
- Vortices are generated at the leading edge of the apertures. Just as in the case of wind tunnel pumping, described in section 2.2, these vortices interact with the trailing edge and this interaction generates acoustic waves, thus enabling a feed-back to the vortex shedding at the leading edge.
- Flow fluctuations caused by the above phenomena may excite acoustic resonances in the cavity behind the apertures.

In reference 9 an alternative (with respect to the standard B&K nose cones) aerodynamic contour has been studied, which was designed to obtain a low pressure gradient in the boundary layer at the screen, see figure 19.

Another aspect investigated in this study is the porosity of the screen. If the flow resistance is high, the fluctuations causing the self-noise are damped. However, the screen should be transparent for the acoustic flow fluctuations, so a compromise has to be found.

Although some improvements have been obtained in the design of quiet nose cones, some problems, such as the sensitivity to cross flows, are not solved yet.

### 4.3 Acoustic arrays

Despite all the efforts to reduce background noise, tunnel wall reflections, and microphone self-noise, an accurate measurement of the sound field in the test section of a wind tunnel can still be a difficult job. Moreover, in many cases researchers not only want to know the sound levels in the field, but also the locations and intensities of the sources.

A method that has the possibilities to deal with both problems is the technique of acoustic arrays. In its most simple application an acoustic array consists of two microphones, with which one can determine the direction of a plane wave impinging on the array. Consider the situation depicted in figure 20. The direction from which the waves are coming (i.e. the angle θ) can be found from the phase difference between the two microphones:

$$\Delta\phi = 2\pi \frac{d}{\lambda} \cos\theta$$

A wrong result is found, however, if more than one wave front passes between the microphones, i.e. if the phase difference is larger than $2\pi$, or $\lambda < d\cos\theta$. The maximum frequency is thus determined by the smallest distance between two microphones.

In the example given here, two microphones are enough to find the direction of the source location. However, in wind tunnel experiments the source usually can not be regarded as being at infinite distance, and the impinging waves will not be plane, in which case an array of more than two microphones is required. Furthermore, often there is not a single point source, but one has to deal with multiple sources or continuous source distributions, in a 3-dimensional setting. In such cases a linear array is not sufficient and 2-D planar arrays should be used. On the software side, the data processing for such systems is much more complicated than the mere application of the equation given above (although the phase differences between the microphones are still at the basis of the computations) and many sophisticated computation methods, in combination with optimized microphone positioning, have been and still are developed to improve the signal-to-noise ratio and the accuracy, see e.g. references 11-13. The result of the data processing is a mapping of the source strength in a specified plane. The maximum frequency at which such an array can be used still depends on the smallest distance between two microphones, whereas the resolution of the mapping depends on the overall dimension of the array and the total number of microphones. Sources which are not in but near the specified plane are detected by the system, but with a lower resolution.

The positioning of such an array can be in-flow or out-of-flow, just as in the case of single microphones. In the case of in-flow positioning of a planar array, additional provisions have to be made to minimize the generation of self-noise, which means that the array has to be embedded in the tunnel wall or in an aerodynamically shaped construction, see reference 14.

The application of an array thus offers the possibility to find noise sources and to distinguish their contribution to the sound field from other components, such as background noise. In principle, acoustic measurements could also be performed in closed wind tunnel test sections with sound-reflecting walls, as an array should be able to distinguish the directly emitted sound from the reflected sound. However, from the literature it is not clear if the state-of-the-art allows for such applications.

# 5 Applications

A complete overview of all applications of anechoic wind tunnels is not possible within these notes. In this section a few typical examples are presented, both within and outside aerospace research.

## 5.1 Propeller Noise

From January 1993 until July 1996 an extensive research project on propellers, sponsored by the European Commission, was carried out by a consortium, consisting of industry, research institutes, and universities, under the name of SNAAP (Study of Noise and Aerodynamics of Advanced Propellers). For this project two six-bladed model propellers of 0.9 m diameter were built, the so-called Low Speed Propeller LSP, design cruise Mach number 0.7, and the High Speed Propeller HSP, design cruise Mach number 0.78. Both propellers were tested in two of the above mentioned wind tunnels: in the ARA-TWT for high-speed tests, and in the DNW for low speed tests. The blades of the model propellers were instrumented with pressure taps, for the measurement of the steady blade pressures, and with Kulites for the measurement of the unsteady components in the blade pressures. In both wind tunnels in-flow microphones (equipped with nose cones, of course) were traversed at sidelines at several radial and angular positions, to obtain a detailed mapping of the sound field.
The pictures in figures 21 and 22 show the HSP in the ARA-TWT and the DNW respectively. Measured and computed sound pressure levels are plotted against the axial coordinate in figures 23 and 24, for a measurement on the LSP in the DNW, and a measurement on the HSP in the ARA-TWT. Considering the size of the models and the frequencies of interest (> 300 Hz) there is no reason to doubt the anechoicity of the DNW. As for the ARA-TWT, the sound levels in the propeller plane plotted against the circumferential angle, see figure 25, show no significant dependency on this angle, despite the rectangular shape of the test section. This is an indication that for this application the anechoicity is of a high quality.

## 5.2 Helicopter noise

One of the obstacles that impede the large scale use of helicopters for civil transport is their noise, which causes public annoyance near heliports in urban areas. The generation of noise by helicopters consists of a number of complicated mechanisms. In figures 26 the components of main rotor noise are shown, indicating that one can distinguish no less than seven different mechanisms. On top of that, noise is also generated by the tail rotor, the aerodynamic interaction between main and tail rotor, the power plant (turbine), and the transmission.
The importance and the complexity of helicopter noise has led to extensive wind tunnel testing in the last decades, especially in the DNW. A typical test configuration is shown in figures 27. An array of microphones is mounted on a support that is aerodynamically shaped and covered

with sound absorbing foam. This support is traversed in streamwise direction, a short distance underneath the helicopter model. The test results can be presented as a contour plot of the sound pressure levels in the plane of consideration. In figure 28 such a contour plot is shown, together with the spectra and time signals measured at two microphone positions.

### 5.3 Airframe noise

With turbofan engines becoming continually quieter, an increasingly important component of aircraft noise is the so-called airframe noise, i.e. the noise that is generated by the interaction of flow with airframe parts, especially protruding parts like the landing gears, flaps, or slats. At this moment the research on airframe noise is one of the most frequent applications of anechoic wind tunnels. Extensive experimental research is also motivated by the fact that airframe noise has a number of broadband components, which are not easily described by analytical or computational methods. The need to detect airframe noise sources and to assess their (relative) strengths, is also the main reason for the current, vivid interest in source location techniques.

In figure 29 a mapping is shown that was obtained in the CEPRA 19 wind tunnel on a one-wing Airbus model, scale 1:11 (Ref. 12). It can clearly be seen that in this case most of the noise is generated at the slats and the landing gear. The scaling of results of model testing to full scale is not always a clear matter, see section 4.1. Therefore, some tests have been carried out on full-scale aircraft components. In figure 30 a picture is shown of the landing gear of an Airbus A320 mounted in the DNW (Ref. 15). For this test a wall was constructed as an extension of the nozzle. The leading edge of this wall was fitted with a scoop to simulate the boundary layer of the lower wing surface. (The boundary layer coming from the nozzle is thicker than the latter.) Furthermore, the cavity in the wing was modelled to obtain, as far as possible, the same sound reflections as with a real aircraft. By testing both the untreated landing gear, and the landing gear partially covered with aerodynamic fairings, an estimate could be made of the potential noise reduction by application of a ‘low noise' design.

### 5.4 High-speed train noise

The noise of conventional trains is dominated by rolling noise, generated by the contact between the wheels and the rails. At speeds higher than 200 km/h, however, aerodynamic sources become more important: the intensity of rolling noise is approximately proportional to $v^3$, whereas aerodynamic noise is proportional to $v^6$, $v$ being the speed of the train. Rolling noise can be screened by acoustic fences, a solution which is impractical for aerodynamic noise suppression, as the sources are distributed over the total height of the train. Indeed, one of the major aerodynamic noise sources is formed by the pantographs (current collectors) at a typical height of 6 m above the track. A recent experiment on the aerodynamic noise of pantographs in the DNW, with use of a 2-D planar array, is reported in reference 13. In figure 31 a sketch of the set-up is depicted, showing the pantograph mounted on a platform which extends from the nozzle, and a planar microphone array just outside the flow. In figure 32 a contour plot of the acoustic intensity is given, together with the position of the pantograph. This so-called acoustic image is the output of an advanced data-processing algorithm, including a ‘principal component analysis' and an ‘adaptive beamforming' technique, which both increase the signal-to-noise ratio, see reference 13.

### 5.5 Car acoustics

In the aeroacoustic research of cars, the emphasis is on interior noise, to increase passenger comfort. In a typical wind tunnel experiment the noise is generated by the hydrodynamic interaction of the flow and the (full-scale) car only (i.e. engine noise and rolling noise are absent) and the noise is measured inside the car. Interior noise problems are caused mainly by (Ref. 16):

- Leakages in door- and window-sealings.
- Flow noise from protrusions, like antennas or side mirrors.
- Flow induced cavity resonances, as in the case of open sun-roofs.
- Local flow separarions, that occur e.g. at the front pillar.

In a wind tunnel experiment the noise caused by the mechanisms mentioned above is contaminated by the tunnel background noise and the noise reflected from the test section walls, which is why also the car industry uses acoustically treated wind tunnels. The tunnel wall reflections seem to be a smaller problem than the background noise. In figure 33 (from Ref. 17) a comparison is made of sound spectra measured in both open and closed test sections, at three different flow speeds; the differences are of minor importance.

The same conclusion can be drawn from a comparison test of 11 European wind tunnels (Ref. 18), in use by the car industry, see table 1. In figure 34 the background noise levels of these tunnels, measured with in-flow microphones, are given. The increase in cabin noise level as a result of a non-zero yaw angle is plotted in figure 35. In wind tunnels with a high background noise level this increase seems to be smaller, because the flow induced noise is hardly of a higher level than the background noise. That tunnel wall reflections are less important follows from the fact that the DNW results appear to be quite good, although they were obtained in the 8 m × 6 m *closed* test section.

## 6 Acknowledgement

The author wishes to thank Mr. H. Holthusen and Mr. J. Kooi (DNW), Mr. A. Julienne (ONERA), and Mrs. M. Wood (ARA) for their help in preparing these notes.

## 7 References

1. Tyler, J.M.; Sofrin, T.G.; Axial Flow Compressor Studies, SAE Transactions, Vol. 70, pp.309-332, 1962.
2. Maruta, Y.; Minorikawa, G.; Developments of Low-Noise Contractive Nozzle used in Acoustic Wind-Tunnel, AIAA Paper 97-1679, 1997.
3. Beranek, L.L.; Sleeper, H.P. Jr.; The Design and Construction of Anechoic Sound Chambers, J. Acoust. Soc. Amer. 18, pp. 140-150, 1946.
4. Easwaran, V.; Munjal, M.L.; Finite Element Analysis of Wedges used in Anechoic Chambers, J. Sound. Vib. 160, pp. 333-350, 1991.
5. Holthusen, H.; Kooi, J.W.; An investigation of low frequency noise and vibration phenomena of the DNW open jet, CEAS/AIAA Paper 95-056, presented at the First Joint CEAS/AIAA Aeroacoustics Conference, Munich, Germany, June 12-15, 1995.
6. Jaeger, S.M.; Allen, C.S.; Soderman, P.T.; Reduction of Background Noise in the NASA Ames 40- By 80-Foot Wind Tunnel, CEAS/AIAA Paper 95-152, presented at the First Joint CEAS/AIAA Aeroacoustics Conference, Munich, Germany, June 12-15, 1995.
7. Blake, W.K.; Mechanics of Flow-Induced Sound and Vibration. Volume I: General Concepts and Elementary Sources, Academic Press, Inc., Orlando, Fla., 1986.
8. Amiet, R.K.; Corrections of Open Jet Wind Tunnel Measurements for Shear Layer Refraction, AIAA-75-532, 1975.
9. Dassen, T.; Holthusen, H.; Beukema, M.; Design and testing of a low self-noise aerodynamic microphone forebody, AIAA-96-1711, 1996.
10. Allen, C.S.; Soderman, P.T.; Aeroacoustic Probe Design for Microphone to Reduce Flow-Induced Self-Noise, AIAA-93-4343, 1993.
11. Johnson, D.H.; Dudgeon, D.E.; Array Signal Processing, Prentice Hall, 1993.
12. Piet, J.F.; Elias, G.; Airframe noise source localization using a microphone array, AIAA Paper 97-1643, 1997.
13. Dassen, A.G.M.; Sijtsma, P.; Holthusen, H.; Van Haaren, R.; Parchen, R.; Looijmans, K.; The noise of a high-speed train pantograph as measured in the German-Dutch Wind Tunnel DNW', presented at the 2nd International Workshop on the AeroAcoustics of High-Speed Trains, Berlin, Germany, 29 and 30 April 1997.
14. Hayes, J.A.; Horne W.C.; Soderman, P.T.; Bent, P.H.; Airframe noise characteristics of a 4.7 % scale DC-10 model, AIAA paper 97-1594, 1997.
15. Dobrzynski, W.; Buchholz, H.; Full-Scale Noise Testing on Airbus Landing Gears in the German Dutch Wind Tunnel, AIAA paper 97-1597, 1997.
16. Dobrzynski, W.; Sources of aerodynamic noise on cars, paper presented at the DGLR-Workshop ‘Aeroacoustics of Cars', DNW, 16/17 November 1992.

17. Jöris, W.; Berneburg, H.; Reintges, R.; Wind noise development of passenger cars in wind-tunnels and on roads, paper presented at the DGLR-Workshop Aeroacoustics of Cars, DNW, 16/17 November 1992.
18. Mercker, E.; Pengel, K.; Lindener, N.; Zacharias, P.; Comparative Investigation of Flow Noise in Wind Tunnels with Different Test Sections, paper presented at the DGLR-Workshop ‘Aeroacoustics of Cars', DNW, 16/17 November 1992.

Table 1 Motorcar wind tunnels

| Wind Tunnel | T.S. Type | Nozzle Area | Contr. Ratio | T.S. Length | Acous. Treat. |
|---|---|---|---|---|---|
| **BMW AG** | 3/4 open | 20.02 sqm | 3.66 | 10.02 m | no |
| **BMW Technik** | 3/4 open | 10.00 sqm | 3.00 | 9.83 m | yes |
| **Daimler Benz** | 3/4 open | 32.64 sqm | 3.60 | 10.00 m | no |
| **DNW** | closed | 48.00 sqm | 9.00 | 20.00 m | yes |
| **FIAT** | 3/4 open | 30.00 sqm | 4.00 | 10.50 m | no |
| **FORD** | 3/4 open | 23.75 sqm | 4.00 | 10.50 m | no |
| **IVK** | 3/4 open | 22.45 sqm | 4.41 | 9.50m | no |
| **Pininfarina** | 3/4 open | 11.75 sqm | 4.00 | 8.00 m | yes |
| **Porsche** | 3/4 open | 22.30 sqm | 6.06 | 13.50 m | no |
| **Porsche** | closed, s.w. | 22.30 sqm | 6.06 | 13.50 m | no |
| **Volkswagen** | 3/4 open | 37.50 sqm | 4.00 | 10.00 m | no |
| **Volvo** | closed, s.w. | 27.06 sqm | 6.06 | 15.82 m | yes |

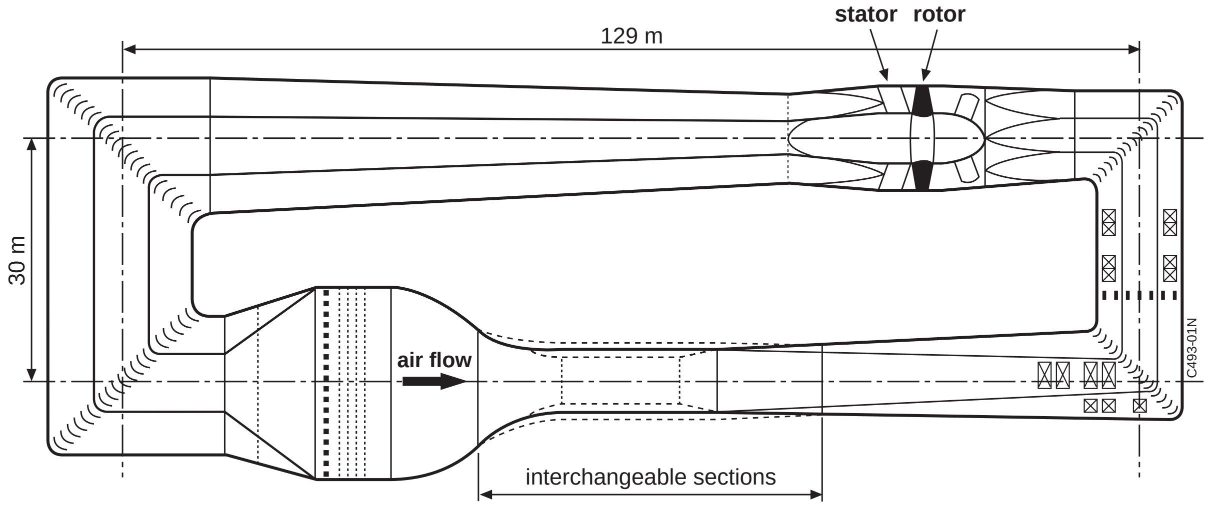


*Fig. 1 Closed circuit wind tunnel with axial fan*

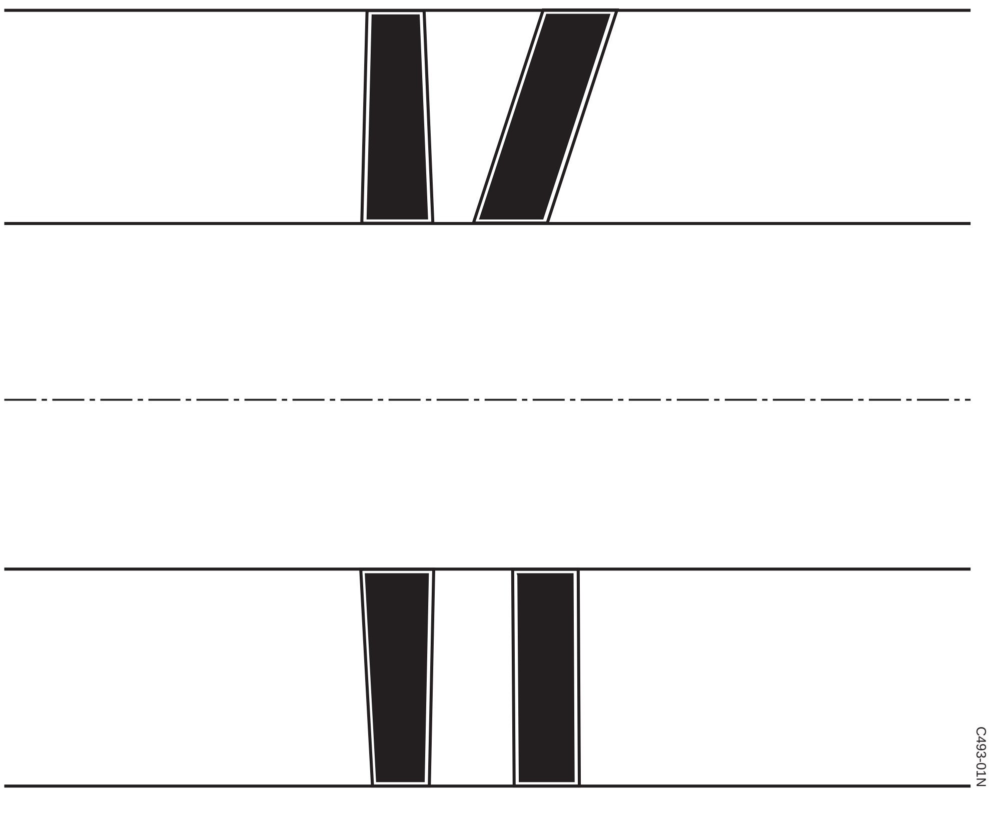


*Fig. 2 Fan geometry: 20 swept stator vane (upper) and unswept vane (lower)*

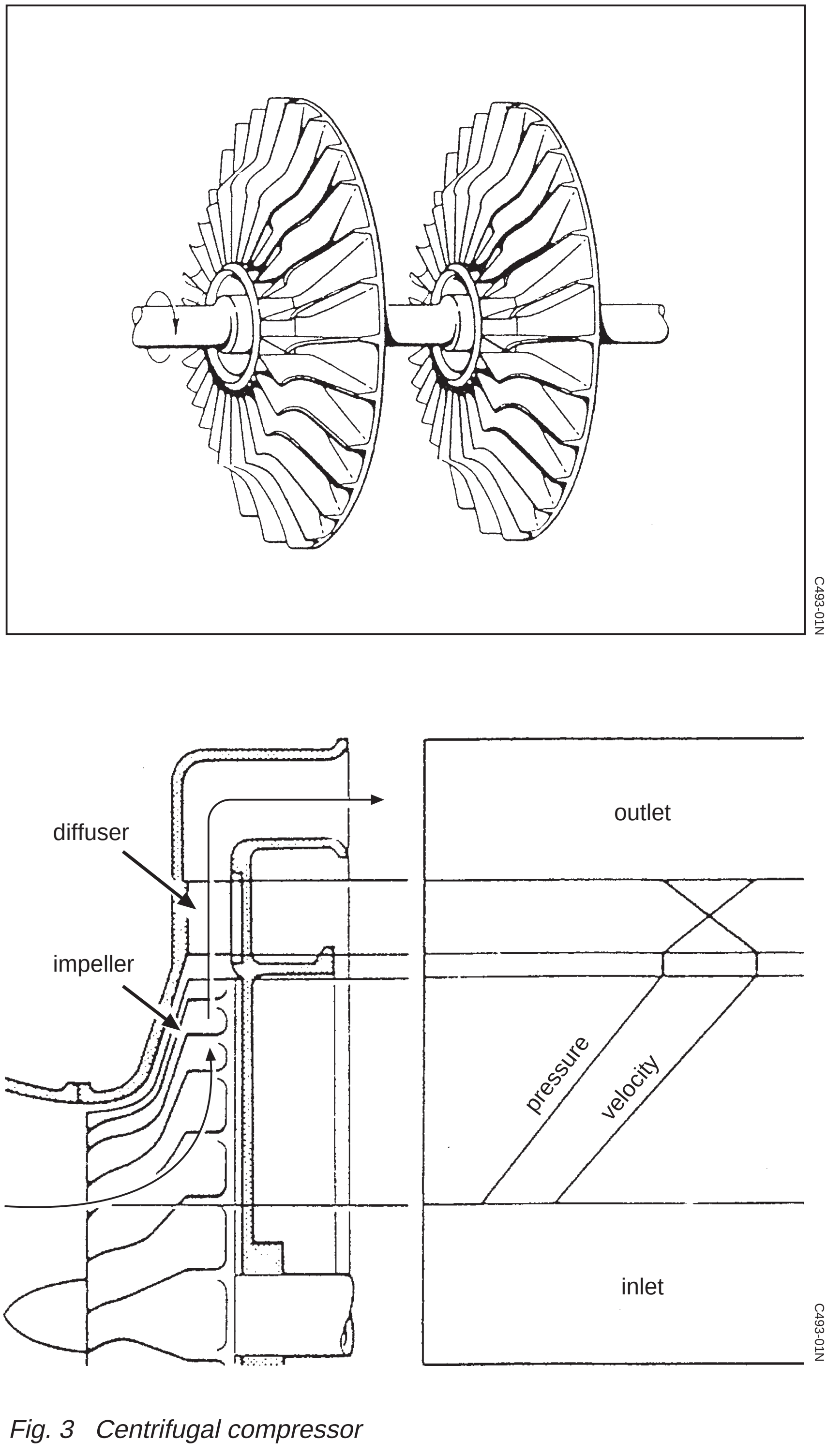


*Fig. 3 Centrifugal compressor*

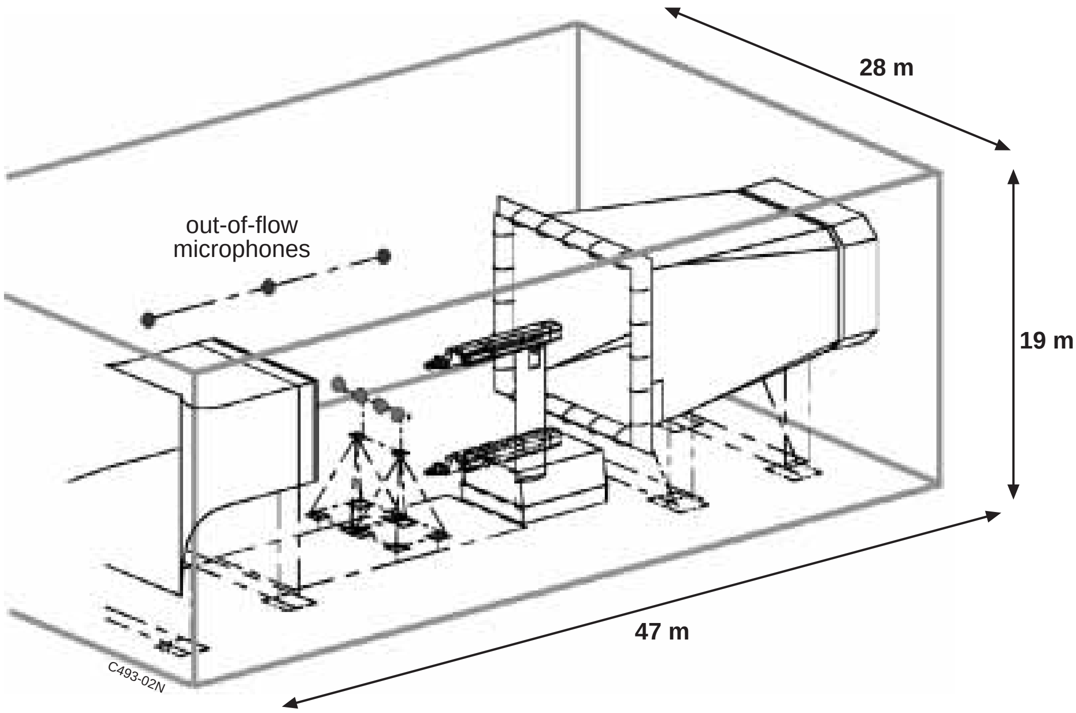


*Fig. 4   Open test section of DNW*

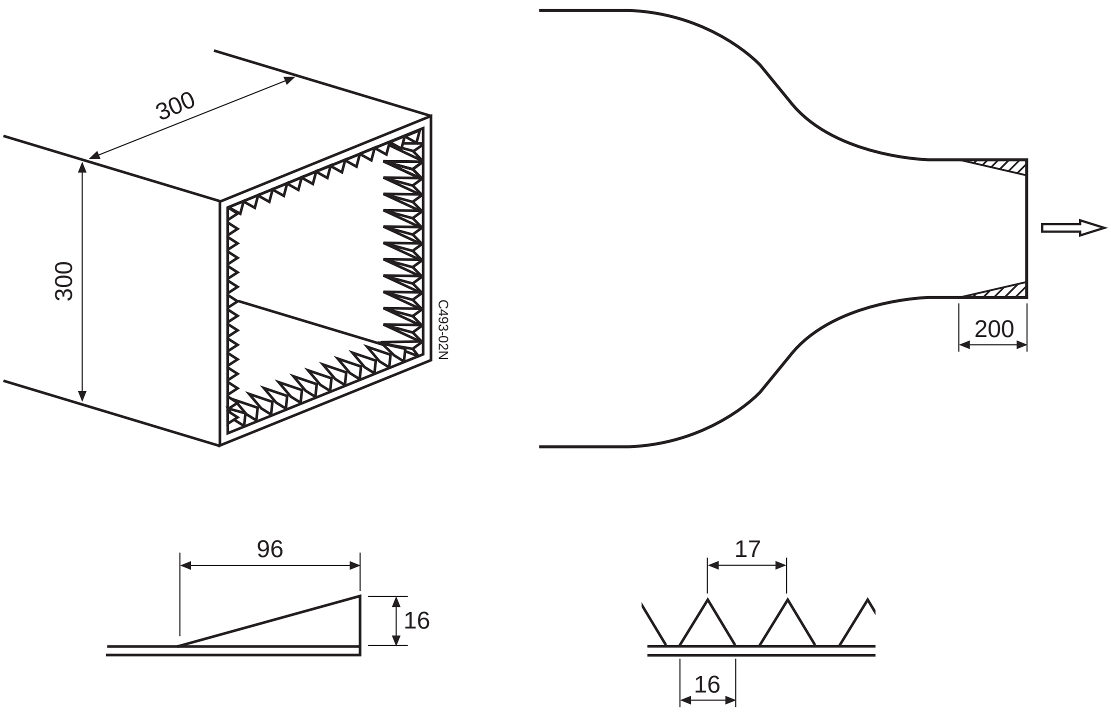


*Fig. 5   Protrusions on nozzle to reduce shear layer noise*

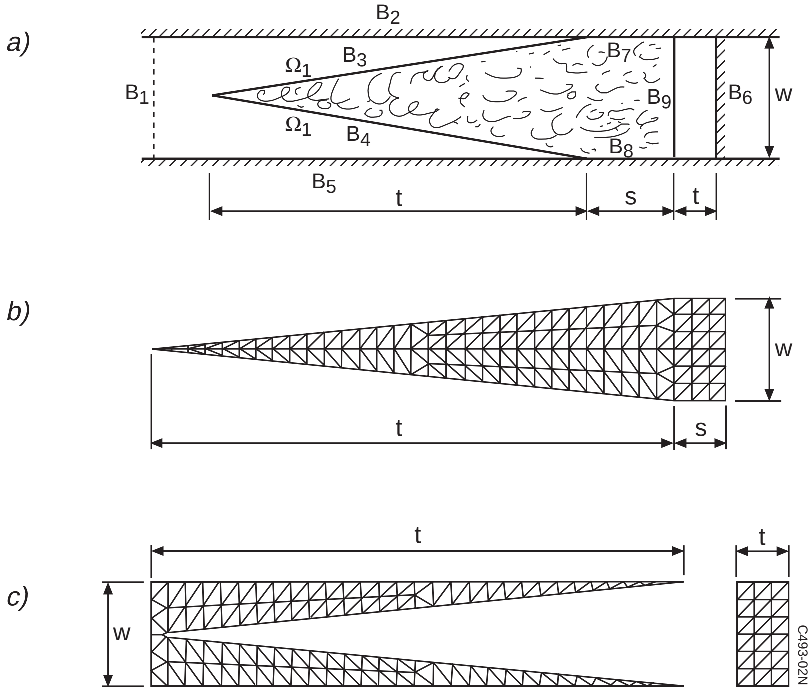


Fig. 6 a) Schematic of a typical wedge;
b) A typical finite element mesh for the wedge;
c) The corresponding mesh in the surrounding medium


Fig. 7 DNW

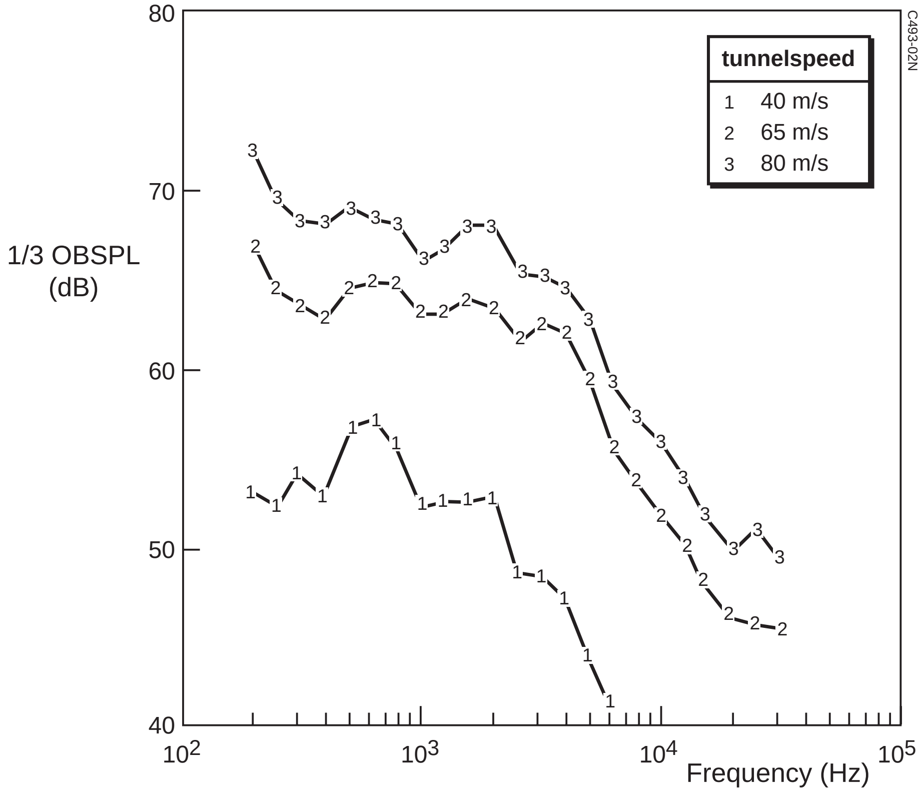


*Fig. 8 Out-of-flow (12.2 m sideline) measured background noise at different tunnel speeds*

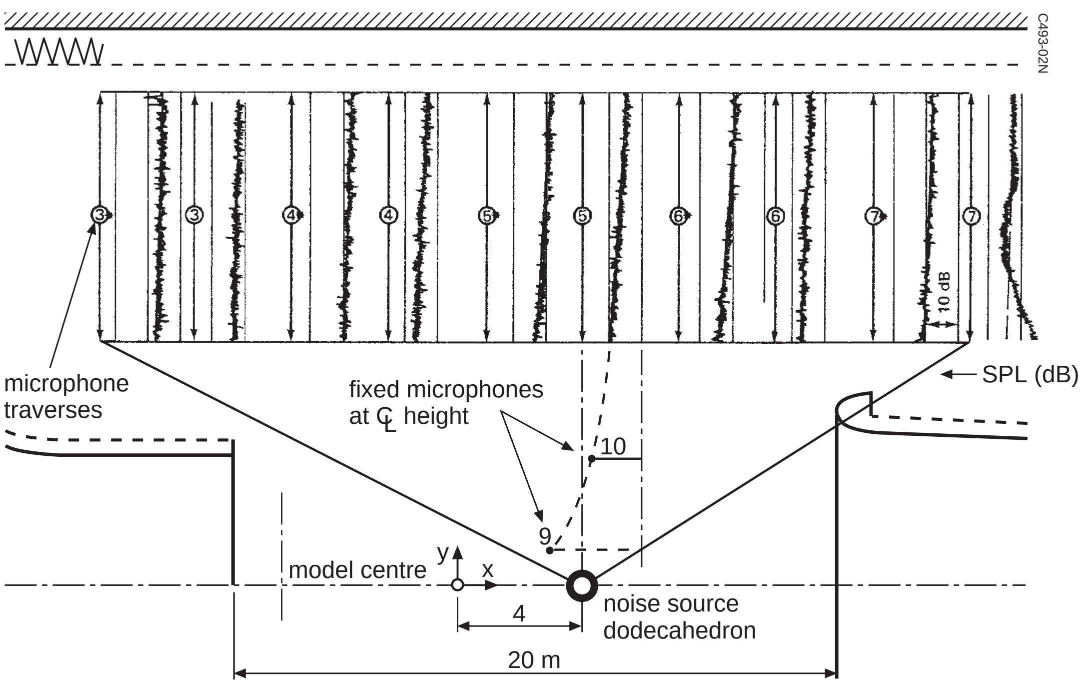


*Fig. 9 l/r$^2$-law test with broadband excitation filtered with 1/3-OB at centre frequency of 400 Hz*

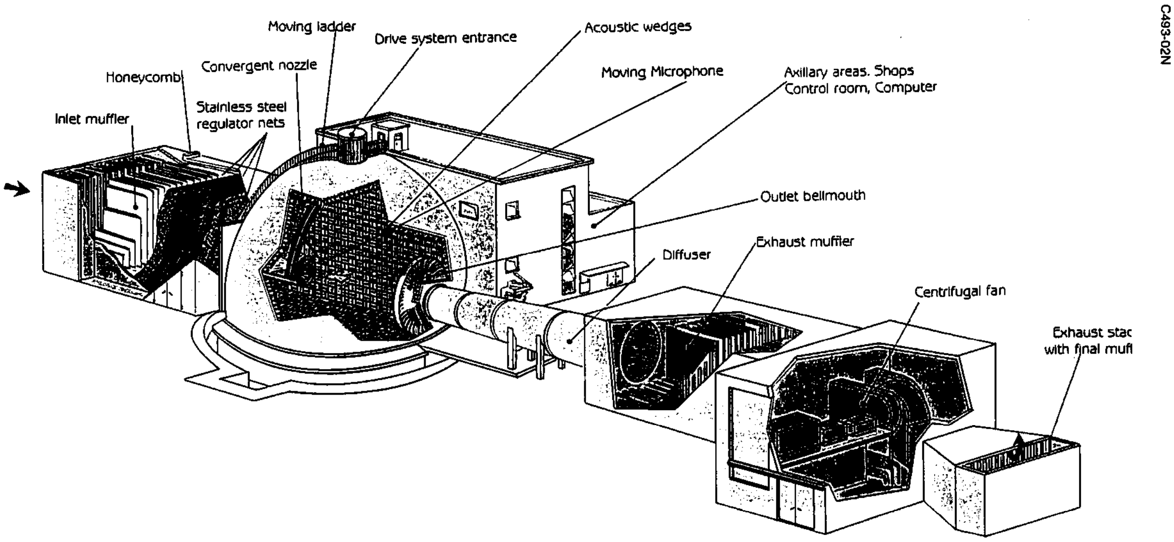


*Fig. 10 CEPRA 19, perspective view from the south*

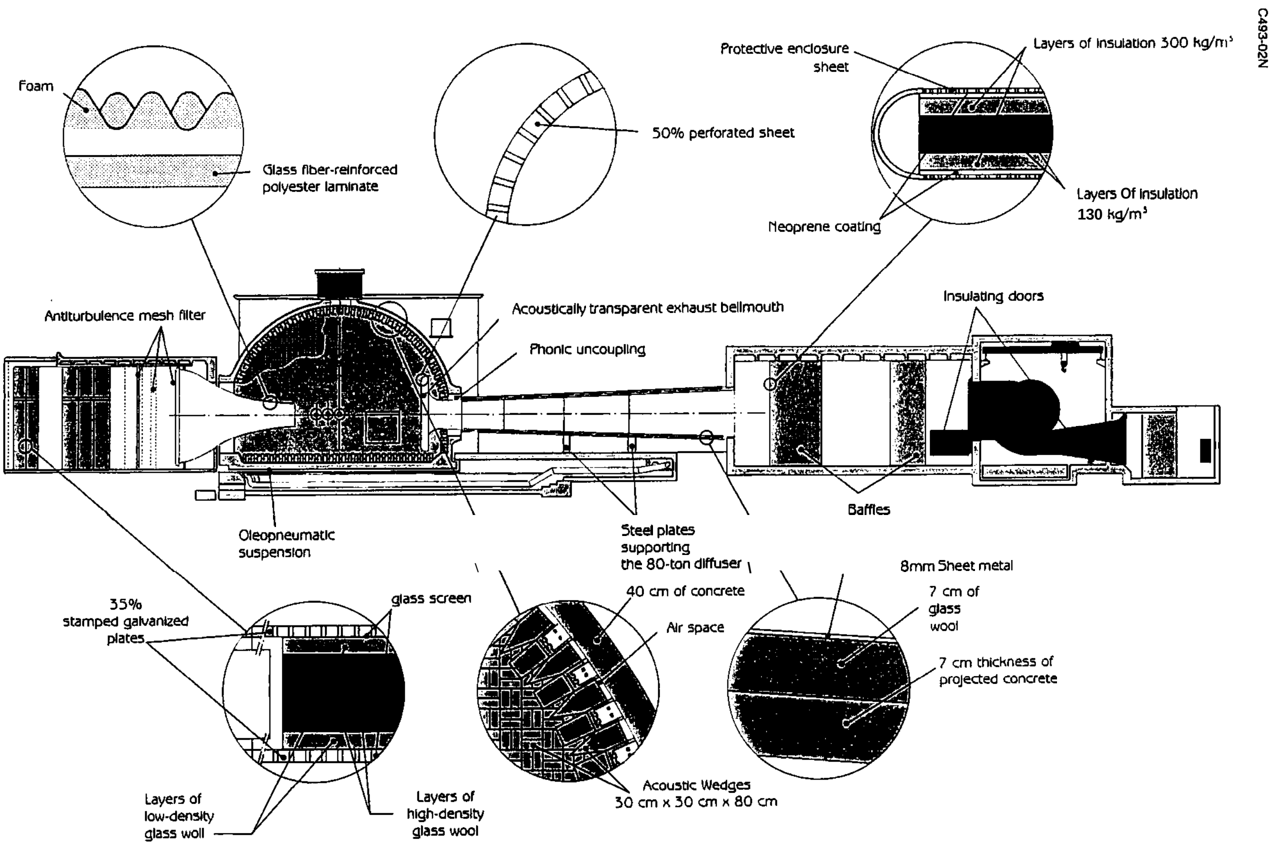


*Fig. 11 CEPRA 19, noise insulation and acoustical treatment*

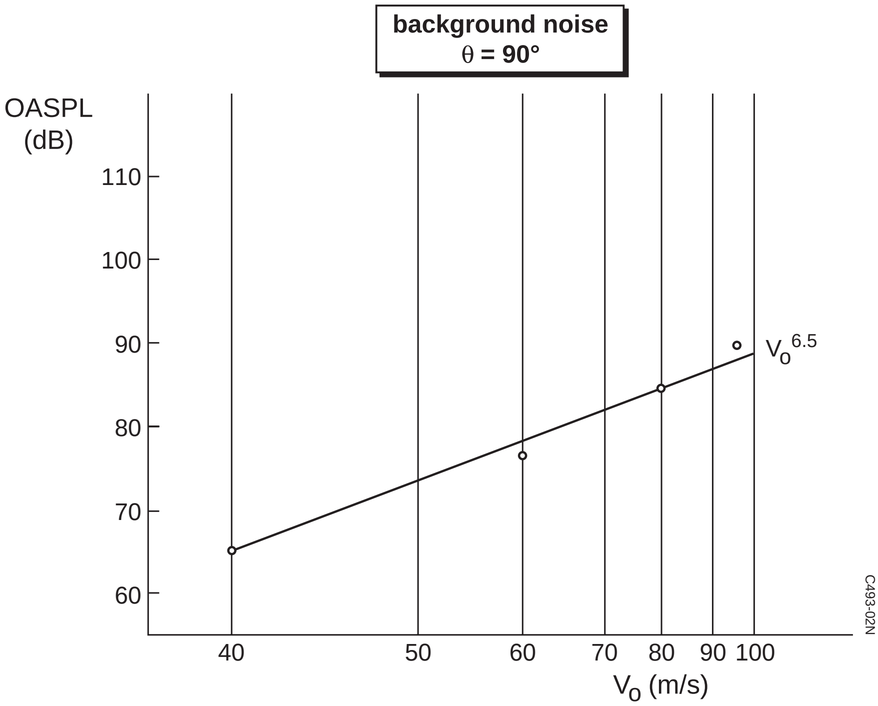


*Fig. 12 Background noise of CEPRA 19*

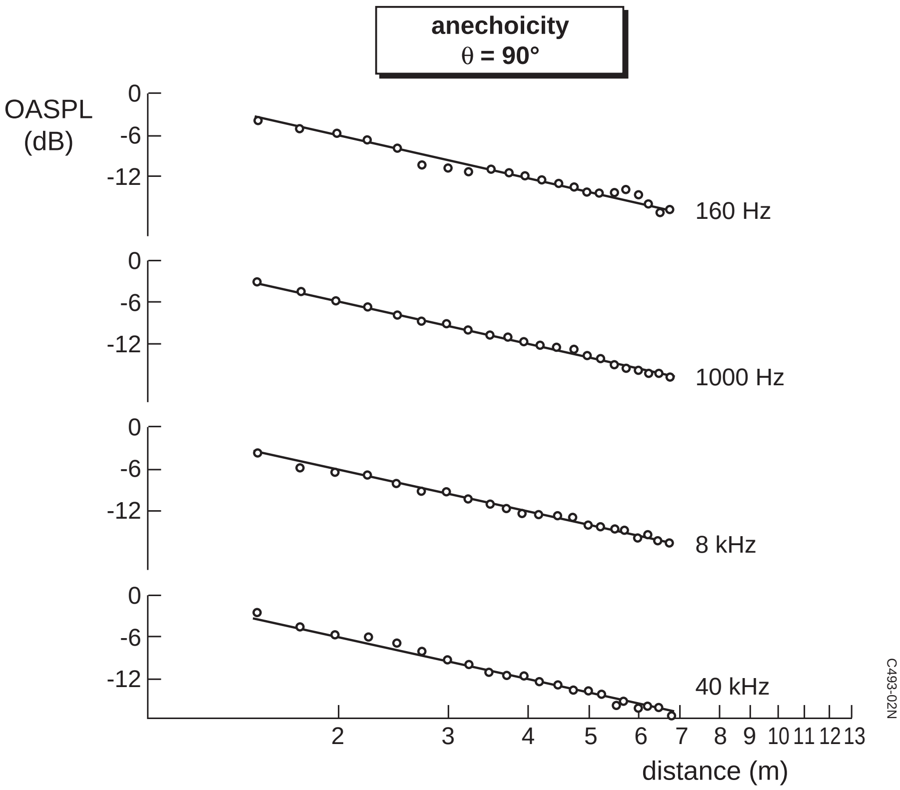


*Fig. 13 Anechoicity of CEPRA 19*

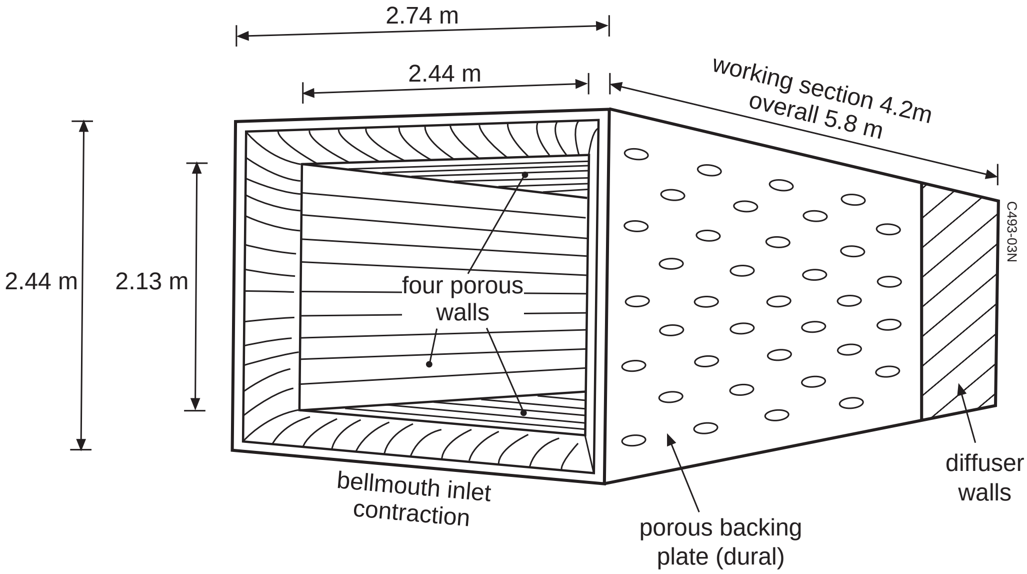


*Fig. 14 Acoustic insert for ARA-TWT*

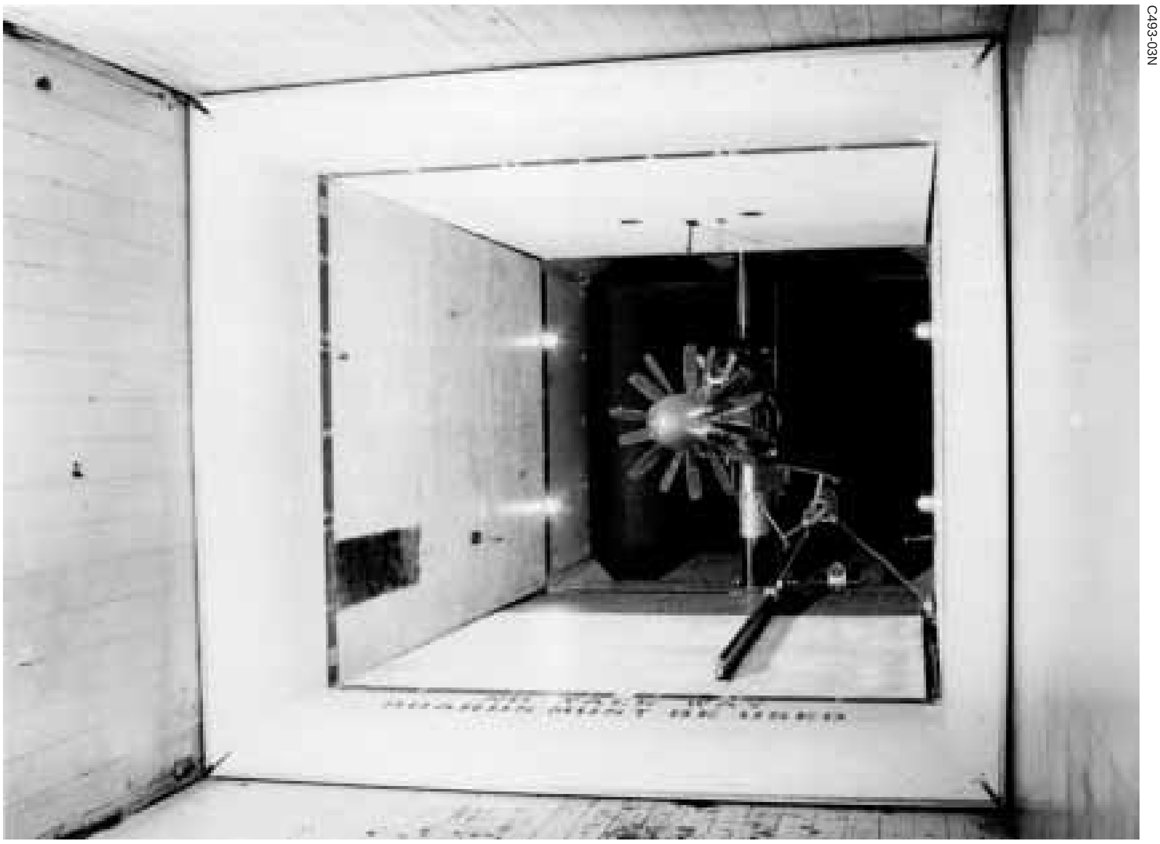


*Fig. 15 Test section of ARA-TWT with acoustic insert*

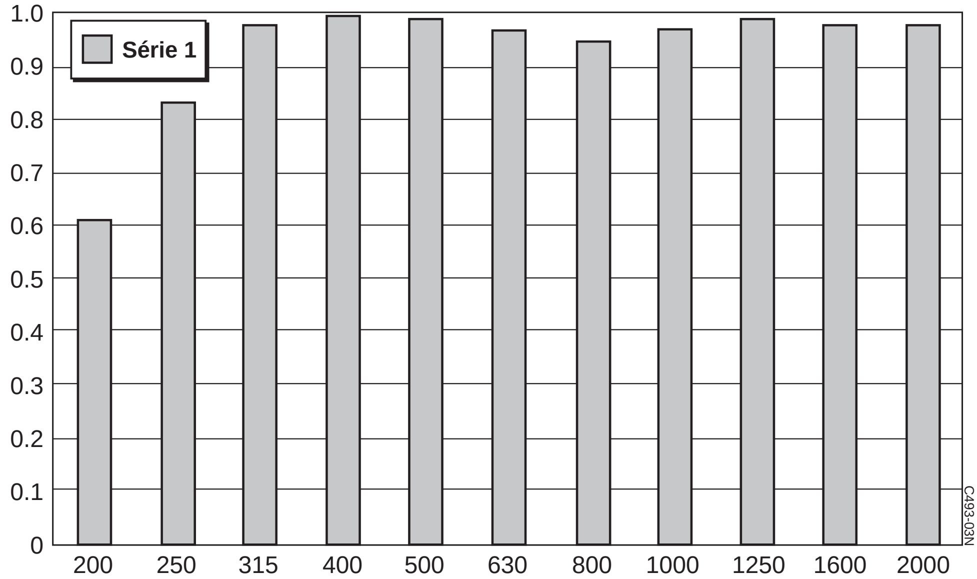


*Fig. 16 Absorption coefficient of acoustic treatment for S1MA for normal waves*

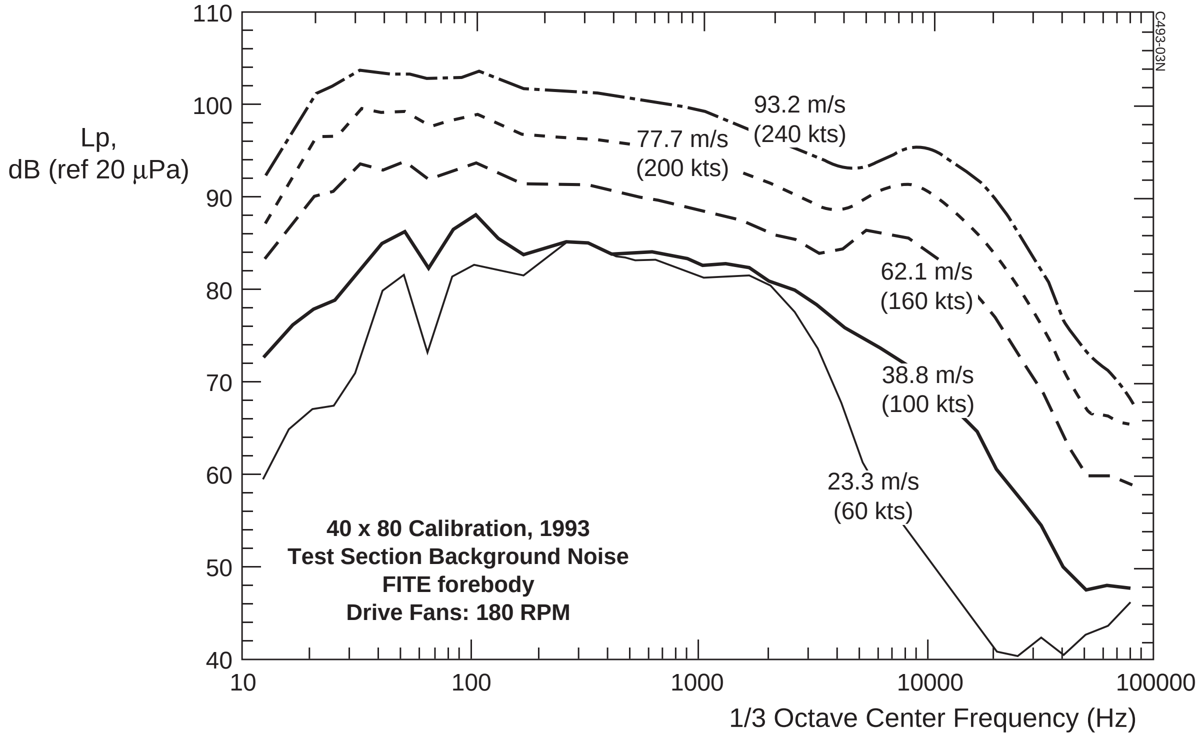


*Fig. 17 NASA Ames 40x80 background noise level vs. frequency for several velocities*

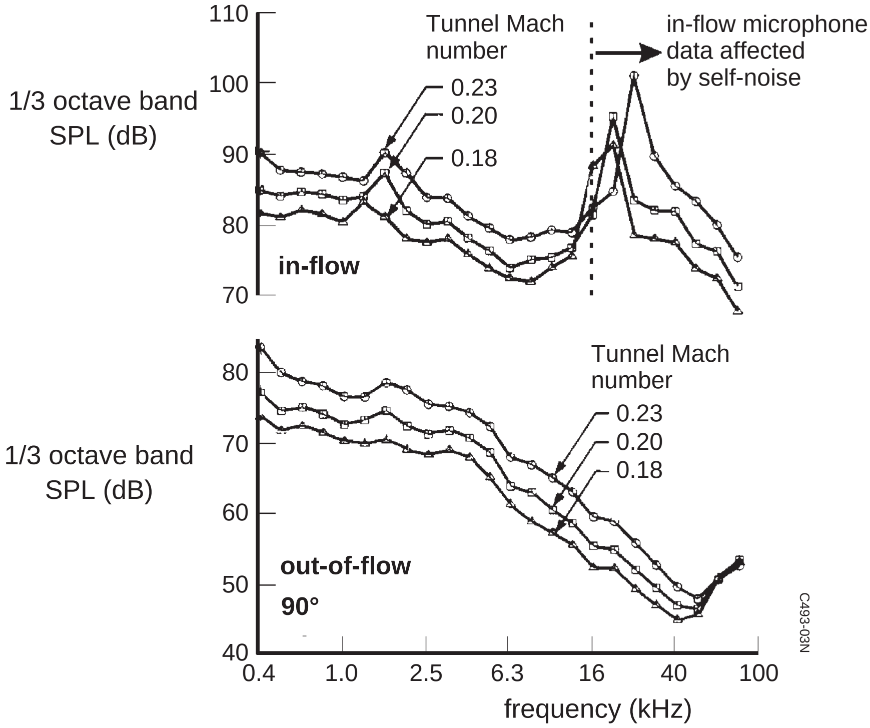


*Fig. 18 DNW background noise levels showing in-flow microphone data affected by self-noise*

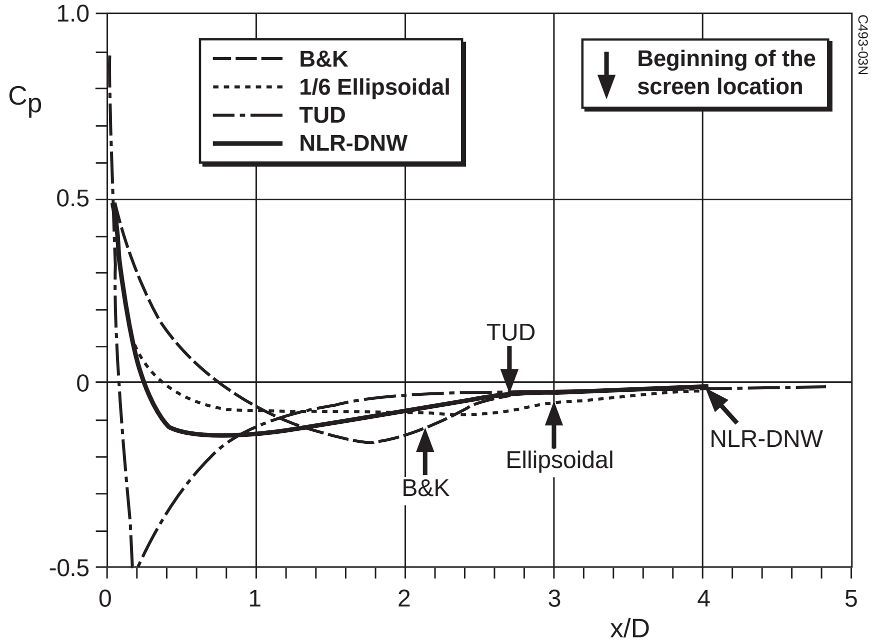


*Fig. 19 Pressure coefficient vs.axial coordinate for several nose cone designs. 'NLR-DNW' is the design of Ref. 9*

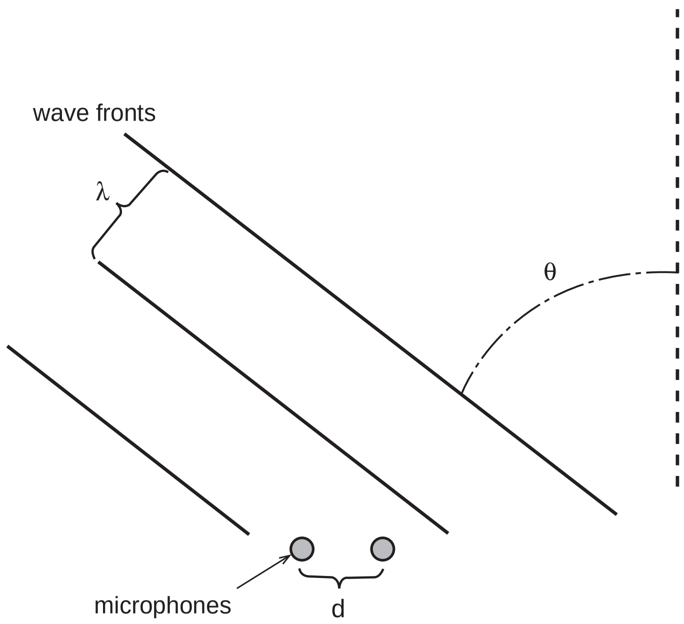


*Fig. 20 Plane wave impinging on array of two microphones*

C493-04N

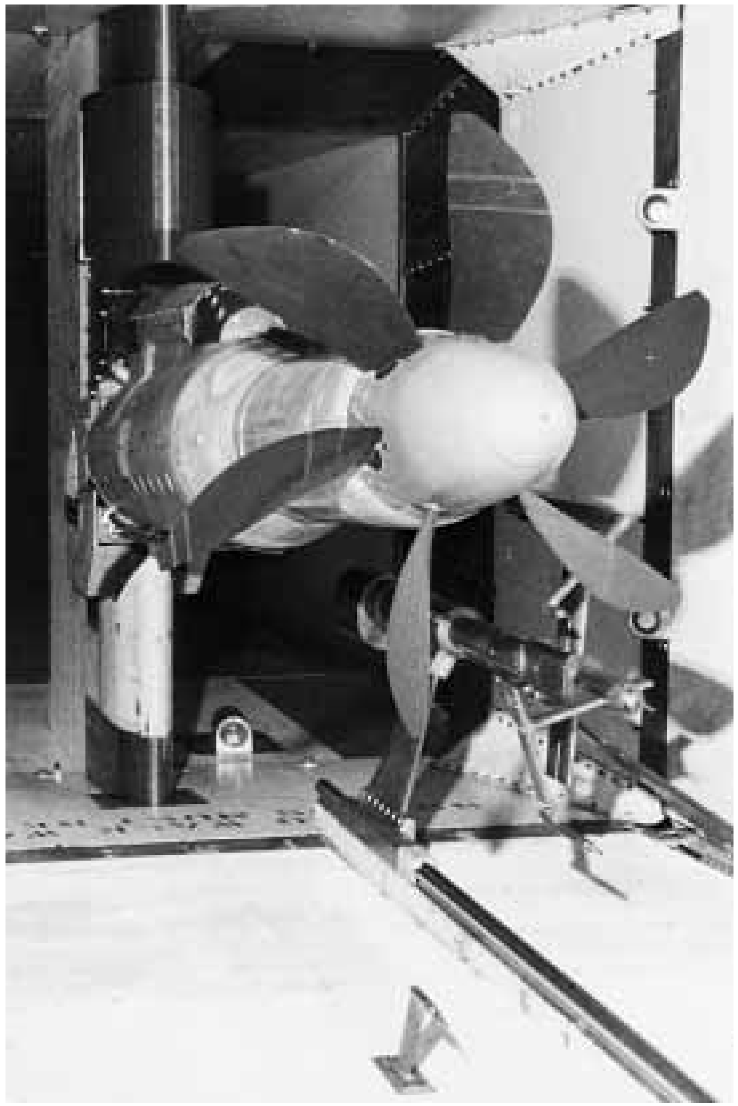

*Fig. 21 SNAAP-HSP in ARA-TWT*

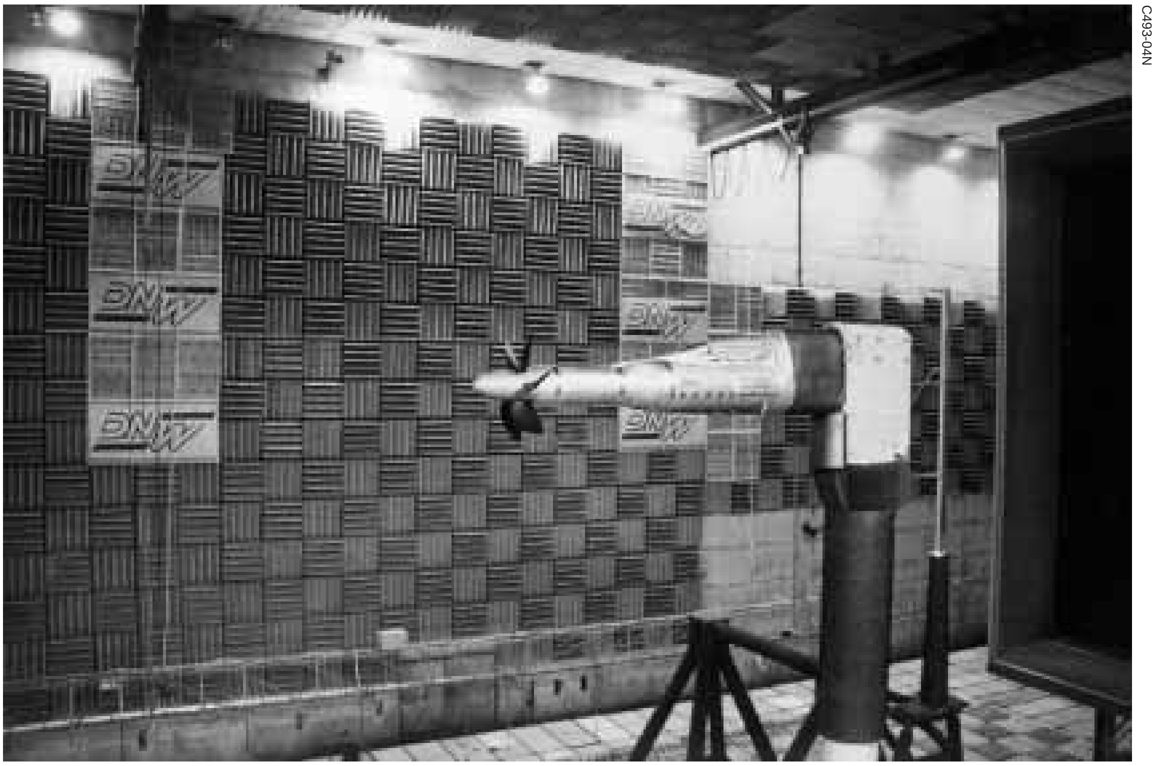


*Fig. 22 SNAAP-HSP in DNW*

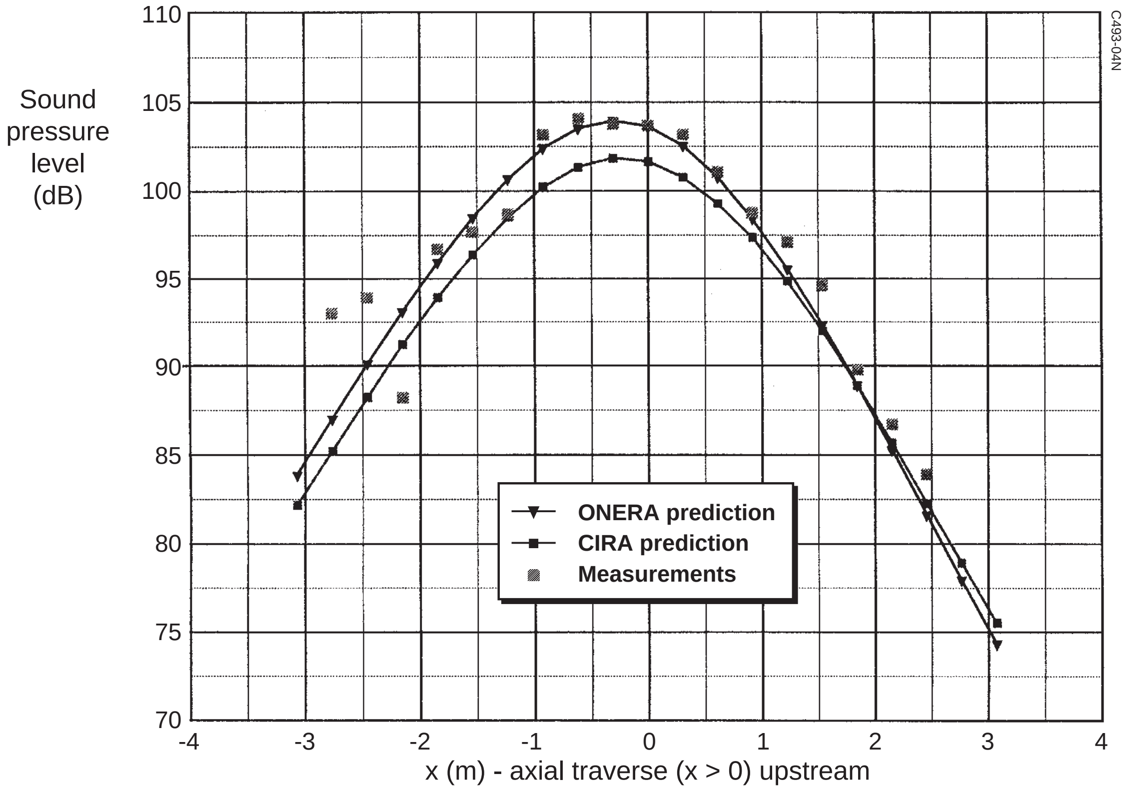


*Fig. 23 Sound pressure level of BPF tone of SNAAP-LSP at Mach 0.2 vs. axial distance*

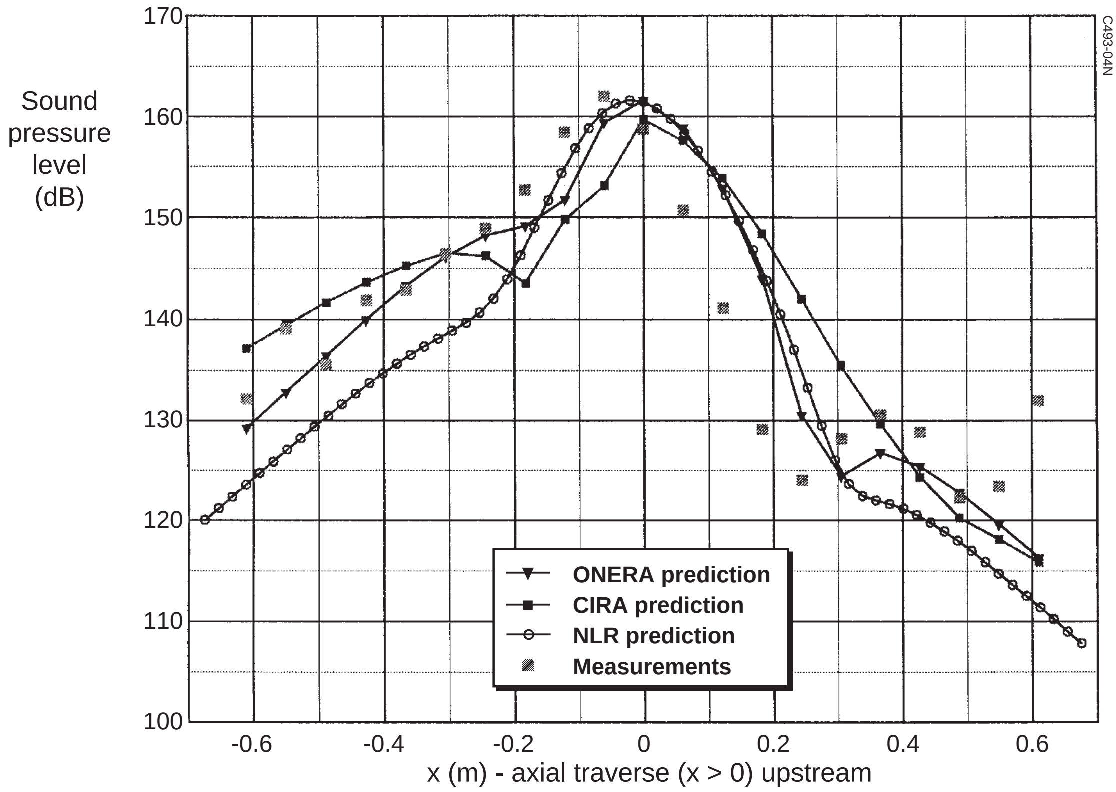


*Fig. 24 Sound pressure level of BPF tone of SNAAP-LSP at Mach 0.78 vs. axial distance*

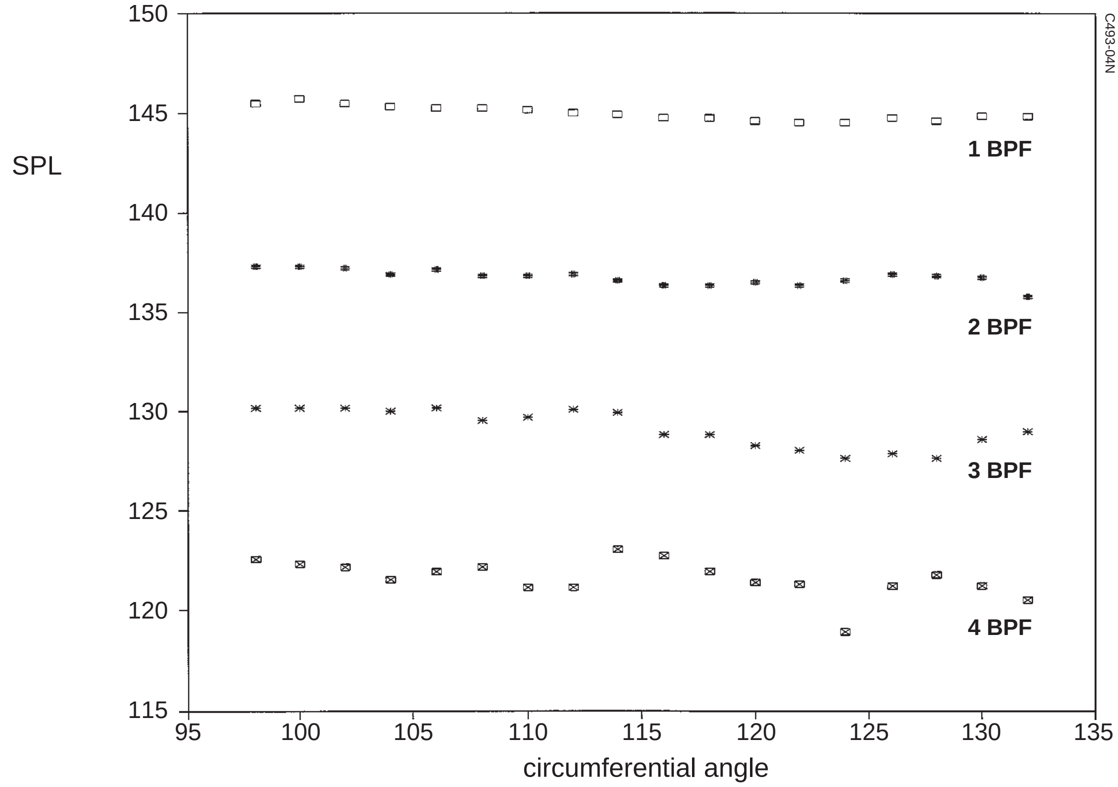


*Fig. 25 Variation of sound pressure level in circumferential direction in ARA-TWT*

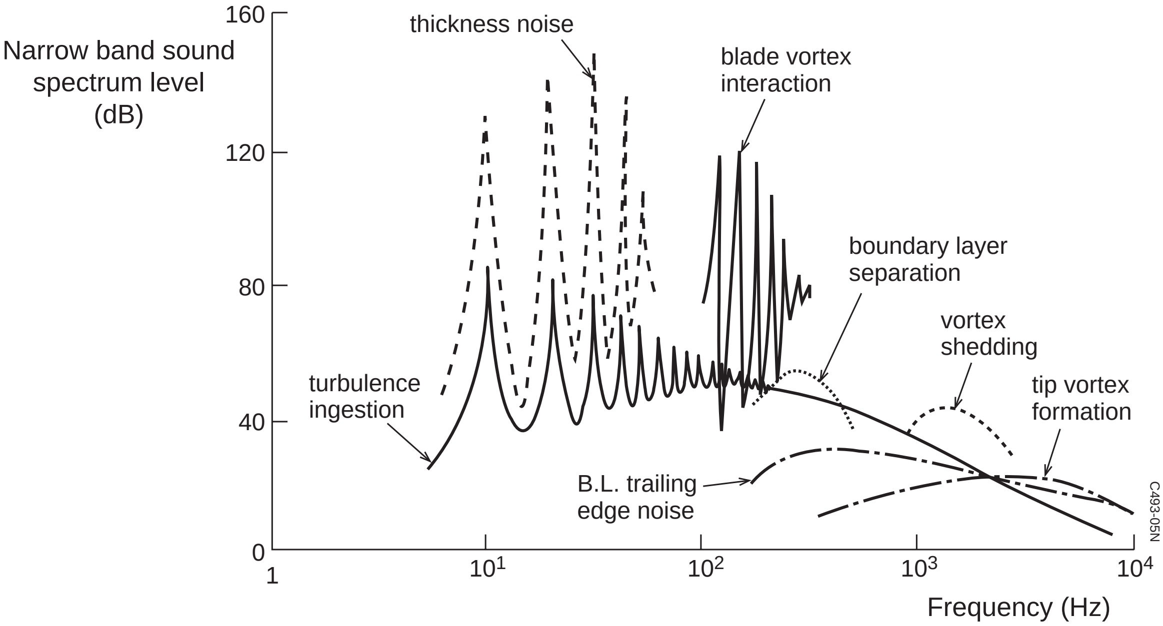


*Fig. 26 Spectrum of helicopter main rotor noise*


*Fig. 27 Helicopter noise test set-up in DNW*

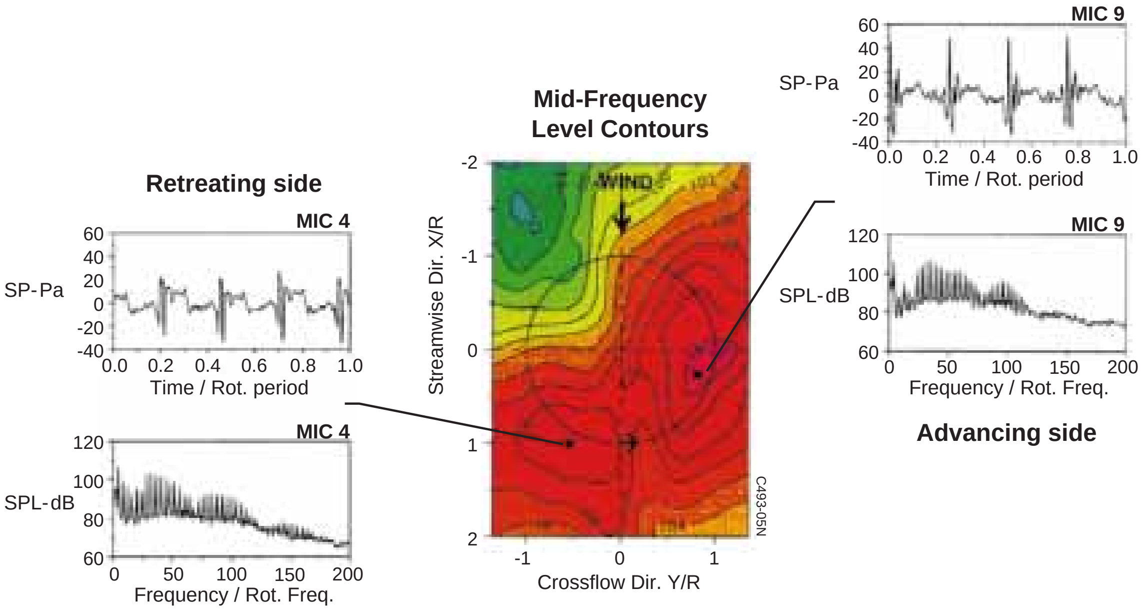


*Fig. 28 Measured noise contours of helicopter main rotor, with spectra and time signals at two microphone positions*

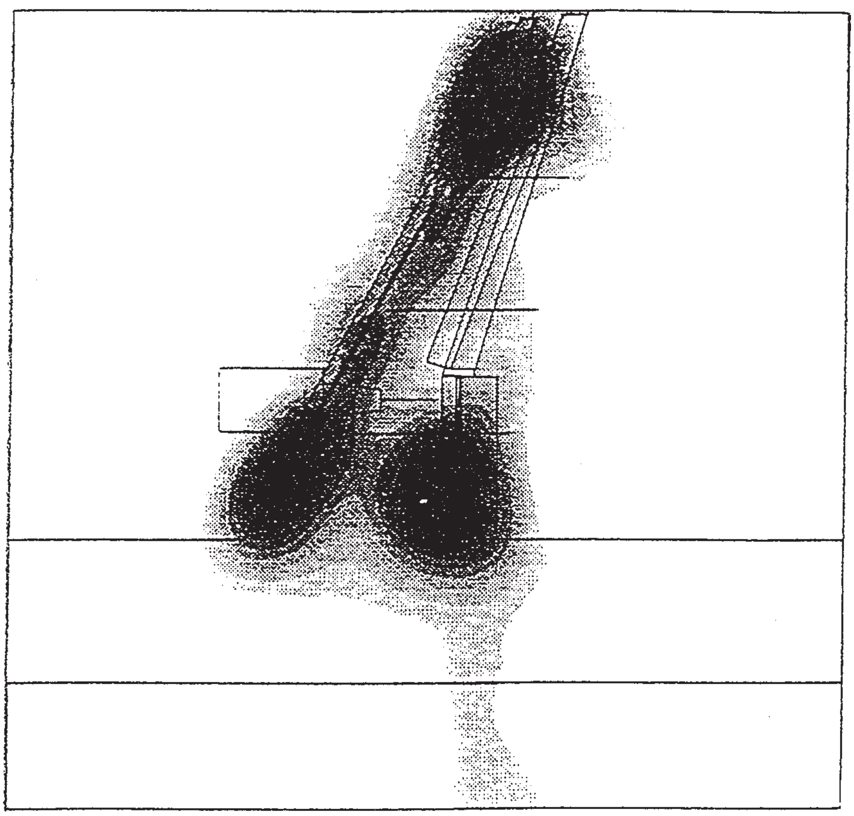

*Fig. 29 Source intensity contours of wing with high lift devices and landing gear*

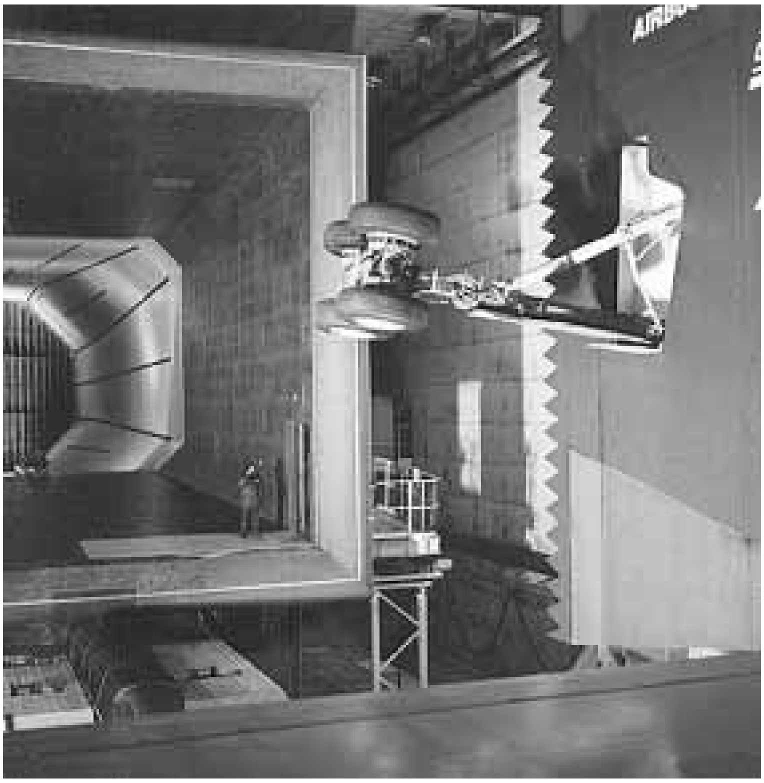

C493-05N

*Fig. 30 Test set-up for landing gear noise*

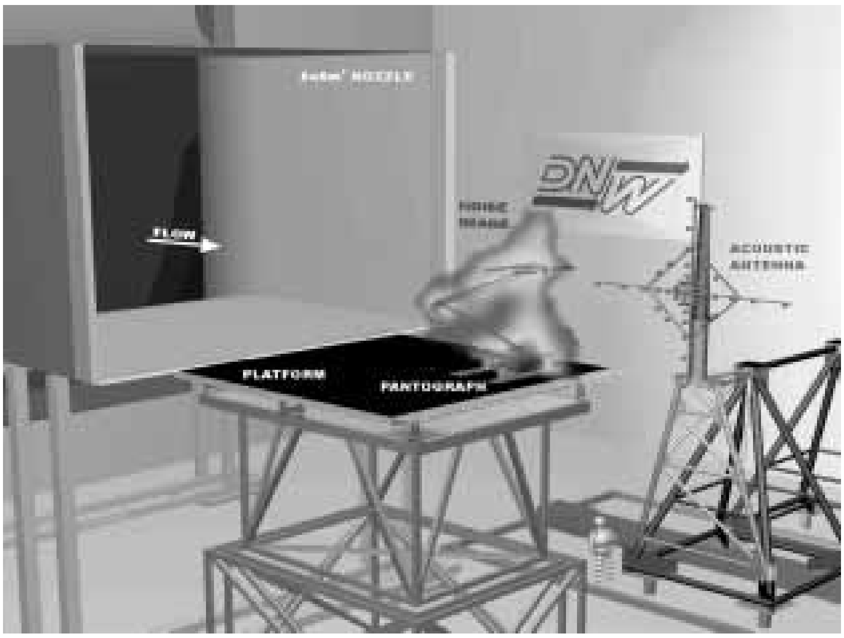


C493-05N

*Fig. 31 Test set-up for directional noise measurements on pantograph*

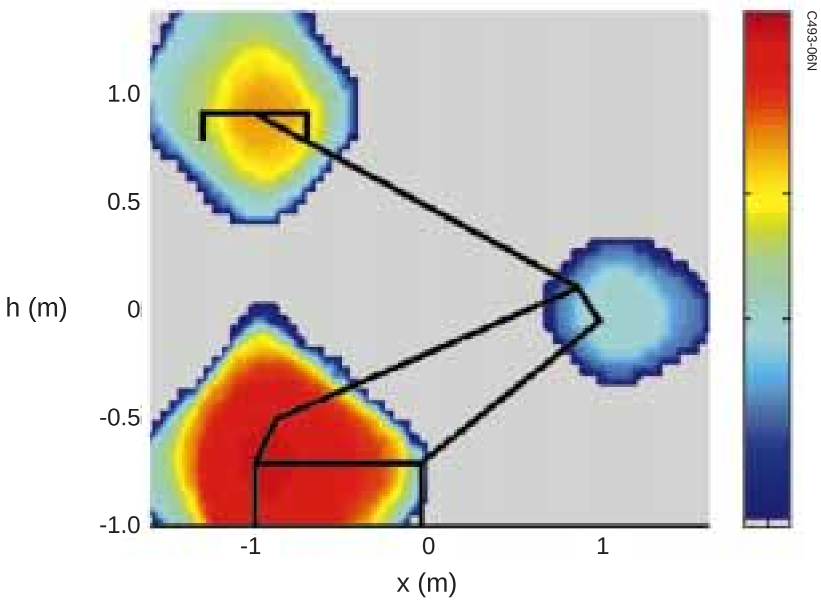


*Fig. 32   Source intensity contours of pantograph*

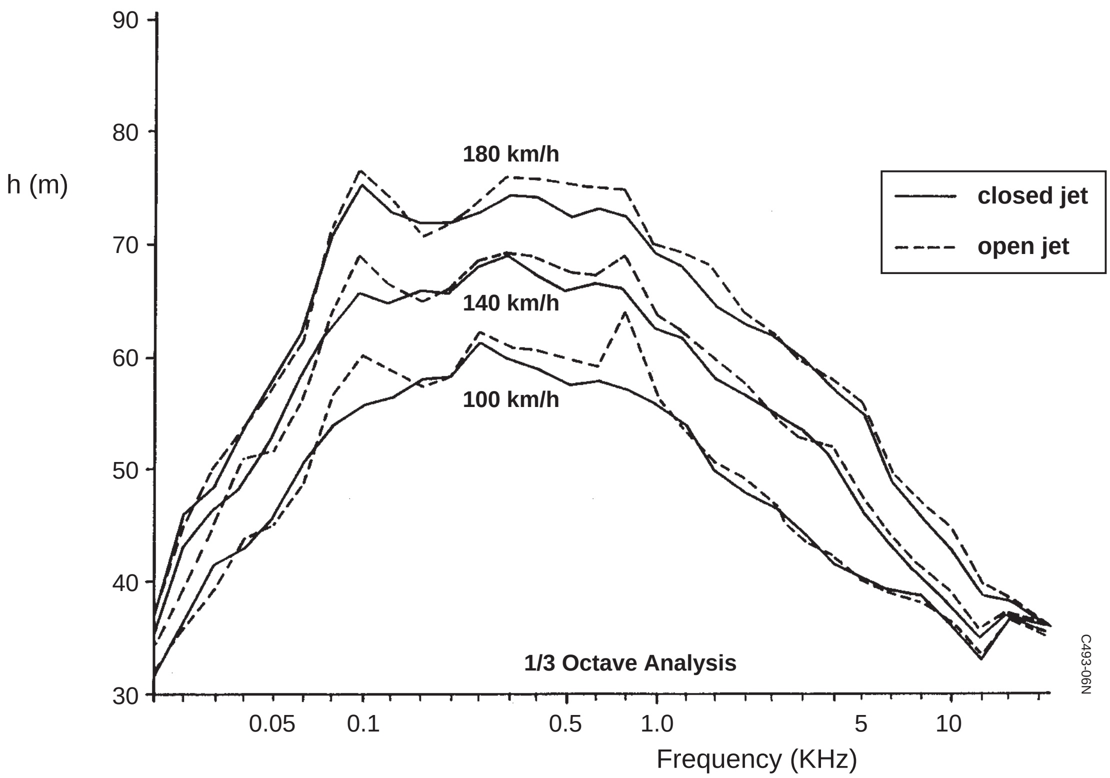


*Fig. 33   Comparison of car interior noise measurements in an open and a closed test section*

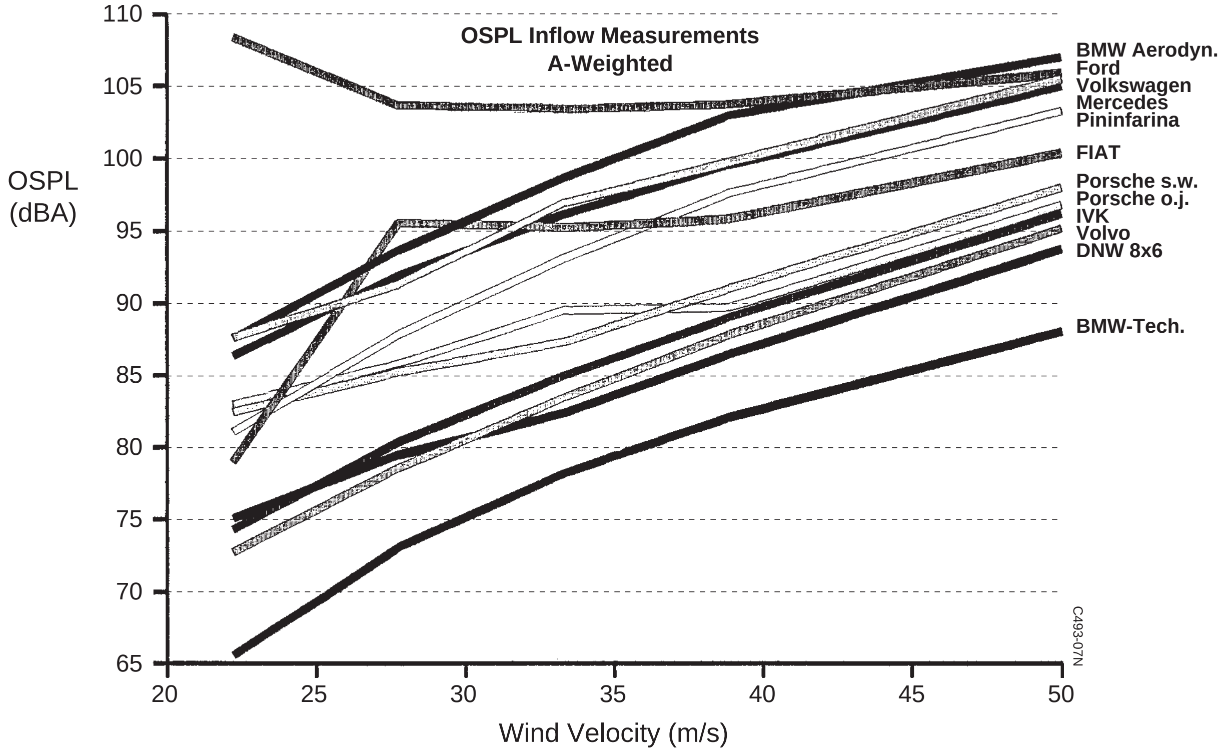


*Fig. 34 Background noise from in-flow measurements of several motorcar wind tunnels*

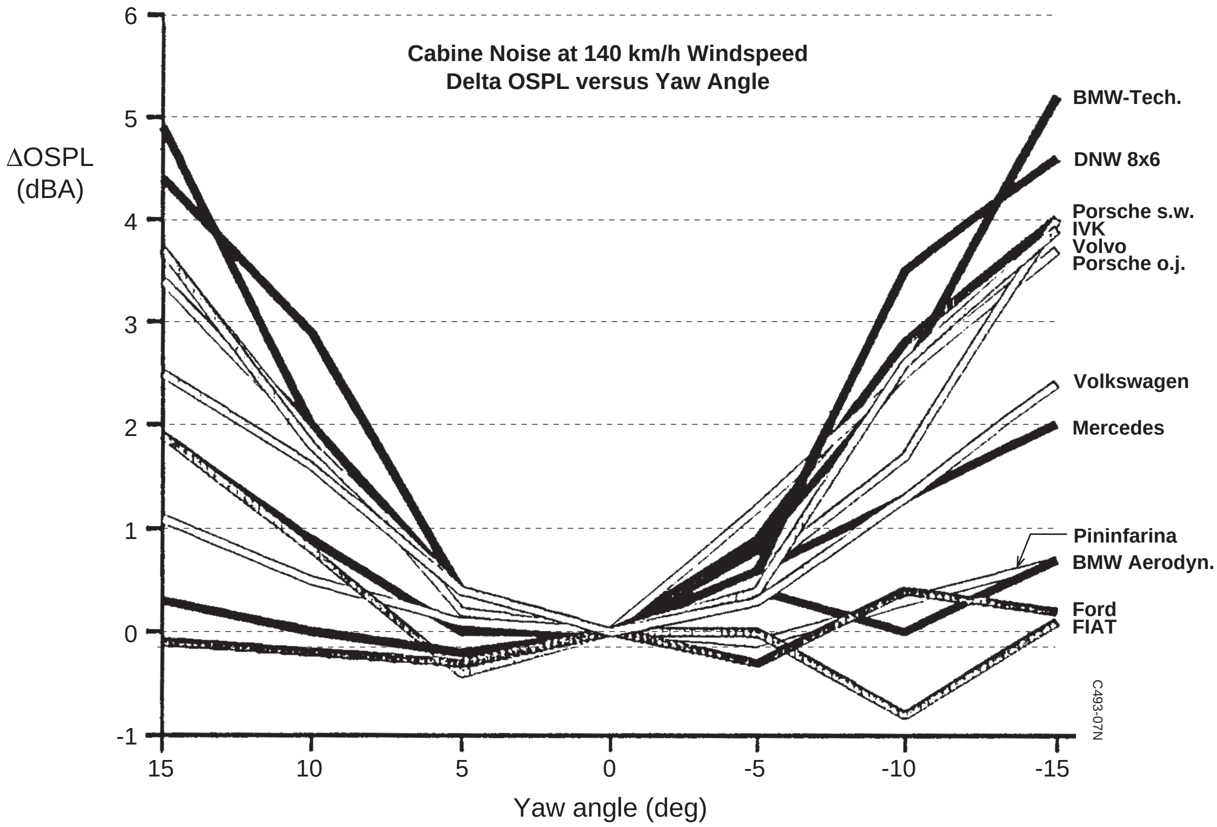


*Fig. 35 Measurement of cabin noise increase due to yaw angle*